Progress in Aerospace Sciences 163 (2026) 101206

Contents lists available at ScienceDirect

Progress in Aerospace Sciences

journal homepage: www.elsevier.com/locate/paerosci

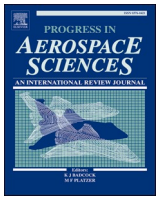

Progress in aerodynamics and aeroelasticity of morphing aircraft

Yuting Dai [a], Jinying Li [a], Yating Hu [a], Jiaying Zhang [a,*], Yuming Zhang [a], Ziyan Xi [a], Yang Zheng [a], Michael I. Friswell [b]

[a] School of Aeronautic Science and Engineering, Beihang University, Beijing, 100191, China
[b] Faculty of Science and Engineering, Swansea University, Swansea, SA1 8EN, UK

A B S T R A C T

This review comprehensively synthesizes the progress concerning the aerodynamic and aeroelastic characteristics of morphing aircraft over the past years (circa 2010-2026). The morphing strategies are categorized into three primary dimensions based on established classifications: chordwise morphing (primarily camber morphing), spanwise morphing (primarily spanwise bending), and planform morphing (including sweep and span morphing). For each morphing strategy, the investigations are systematically reviewed, detailing advances in steady and unsteady aerodynamics, aeroelastic modeling and characteristics, and the application of active control strategies (aeroelastic and maneuver control). Distinct research priorities exist for different morphing strategies: chordwise camber morphing focuses primarily on aerodynamics, while spanwise bending centers on aeroelastic modeling and characteristics. Moreover, given the potential application in configuration adjustments across different flight phases, research on sweep and span morphing predominantly focuses on steady and quasi-steady states. The review also summarizes the current methodologies employed in aerodynamic and aeroelastic analysis and highlights the primary approaches for incorporating aerodynamic (primarily computational fluid dynamics) and structural nonlinearities, as well as their interaction frameworks, such as coupling with computational structural dynamics. The implementation of morphing in control systems is also reviewed, where a notable trend is the integration of control law modules (primarily feedforward and feedback control) into fluid–structure interaction frameworks. As a conclusion, the gap between model and practical application for morphing aircraft still exist. The challenges of detailed modelling for actuation system and time-varying aerodynamics should be paid more attention.

1. Introduction

Morphing aircraft has gained significant research interest over the past decade. It dynamically adjusts its aerodynamic configuration to optimize performance across different flight phases and environmental conditions [1]. Numerous experiments and numerical results have demonstrated that morphing structures can enhance aerodynamic efficiency, reduce fuel consumption, and increase multi-mission versatility. Various morphing strategies offer specific advantages, such as suppressing flow separation with camber morphing and increasing the flutter boundary through spanwise bending.

Among many forms of classification of morphing strategies, the most common one is to classify them according to morphing degrees of freedom [2,3]: airfoil (camber and thickness), wing (twist, spanwise bending, gull, and dihedral), and aircraft planform (span and sweep). The morphing classification and schematics are shown in Fig. 1.

Early in the 1900s, the Wright Brothers applied roll control via twist morphing to the first powered air vehicle [4]. Over the past few decades, research on the structure, aerodynamics, and aeroelasticity of morphing has never ceased. With the development of materials technology and the progress of numerical simulation and wind tunnel research methods, the research on morphing has gradually matured, especially for camber morphing and spanwise bending. In this context, several review papers have been published to summarize the recent progress in morphing research. **Ajaj et al (2021)** [2] provided a comprehensive review of the aeroelasticity of morphing aircraft, with a particular emphasis on structural modeling approaches and aeroelastic coupling mechanisms. More recently, **Mowla et al. (2025)** [5] paid particular attention to control strategies, which are systematically classified and discussed their respective merits and limitations, offering a structured picture of how morphing systems can be controlled across different contexts. Complementarily, **Parancheerivilakkathil et al. (2024)** [3] focused on especially AI-driven approaches to morphing technologies and further discussed the potential industrial applications and future directions. Compared with former reviews, the present paper places greater emphasis on the aerodynamic studies of morphing technology. Specifically, it categorizes various morphing concepts and systematically reviews their impacts on steady and unsteady aerodynamics, aeroelastic modeling, and control, with particular attention to the nonlinear aerodynamic characteristics induced by morphing. This perspective provides a physics-based foundation that complements the structurally oriented, control-oriented, and industrial-oriented reviews in the existing literature.

* Corresponding author.
E-mail address: jiaying.zhang@buaa.edu.cn (J. Zhang).

https://doi.org/10.1016/j.paerosci.2026.101206
Received 18 January 2026; Received in revised form 17 March 2026; Accepted 28 March 2026
Available online 8 April 2026

Abbreviation

ACTE	Adaptive Compliant Trailing Edge
AoA	Angles of Attack
ASTA	Adaptive Super-Twisting sliding mode Algorithm
CFD	Computational Fluid Dynamics
CSD	Computational Structural Dynamics
DES	Detached Eddy Simulation
DNS	Direct Numerical Simulation
FEM	Finite Element Method
FishBAC	Fish-Bone-Active Camber
FSCI	Fluid-Structure-Control Interaction
FSI	Fluid-Structure Interaction
GRA	Green Regional Aircraft
INDI	Incremental Nonlinear Dynamic Inversion
LE	Leading Edge
LEV	Leading Edge Vortex
MAVs	Micro Aerial Vehicles
NMI	Nonlinear Model Inversion
RANS	Reynolds-Averaged Navier-Stokes equations
ROM	Reduced-Order Modeling
SMAs	Shape-Memory Alloys
TE	Trailing Edge
TEV	Trailing Edge Vortex
UAV	Unmanned Air Vehicle
VCCTEF	Variable Camber Continuous Trailing Edge Flap
VLM	Vortex Lattice Method

Significant research on structural design, aerodynamic simulation, wind tunnel test verifications, and even flight tests have been done on trailing-edge (TE) camber morphing. Woods et al. [6–9] propose a continuous camber morphing trailing edge called fish-bone-active camber (FishBAC), as shown in Fig. 2(a), and conduct a series of numerical and wind tunnel investigations. There are also many projects supported by the government and companies. In the Adaptive Compliant Trailing Edge (ACTE) project [10], as shown in Fig. 2(b), a Gulfstream III aircraft with a seamless camber morphing trailing edge is adopted for the flight tests to verify the feasibility and deflection capability of the morphing trailing edge. In the Mission Adaptive Compliant Wing (MACW) project [11–14], flight tests on an Unmanned Air Vehicle (UAV) are carried out to reduce drag and decrease fuel consumption by camber morphing.

Spanwise bending is also a promising morphing strategy that has received much research attention in recent years, especially the folding wingtip. As shown in Fig. 3(a), the folding wingtip is adopted on the Boeing 777X [15] to balance the airport space and aerodynamic performance, although this application does not involve the dynamic morphing process during flight. As shown in Fig. 3(b), the Albatross ONE [16] of Airbus is a recent example of a passive folding wingtip, aiming to alleviate the dynamic loads.

The common strategy for sweep morphing is the rotary-variable sweep (RVS) [17], which changes the sweep angle by rotating the wing root around an axis. It is applied to F-111 and F-14 [18]. For other morphing strategies, due to the balance between the difficulty of structure implementation and aerodynamic performance improvement, research is relatively scarce, and the technology is not yet mature.

The conceptual foundation of morphing aircraft lies in their ability to dynamically adapt aerodynamic configurations during flight. However, current research efforts remain predominantly focused on static aerodynamic analysis and the mechanical realization of morphing mechanisms. Research on unsteady aerodynamic and aeroelastic characteristics during dynamic morphing is also critical for morphing aircraft.

In Section 2, the paper introduces and summarizes the development of aerodynamics and aeroelasticity. The morphing strategies are classified into three types, as shown in Fig. 1, corresponding to Sections 2.1, 2.2, and 2.3. Then, the aerodynamic and aeroelastic numerical methods and the active control are classified in Section 3.

2. Development of aerodynamics and aeroelasticity for morphing wing/aircraft

In this chapter, different sections represent morphing platforms, including airfoils, wings, and aircraft. The detailed classification is shown in Fig. 1. The development of aerodynamics and aeroelasticity of morphing is classified into steady aerodynamics, unsteady aerodynamics, aeroelasticity (including aeroelastic model and characteristics), and active control (including aeroelastic control and maneuver

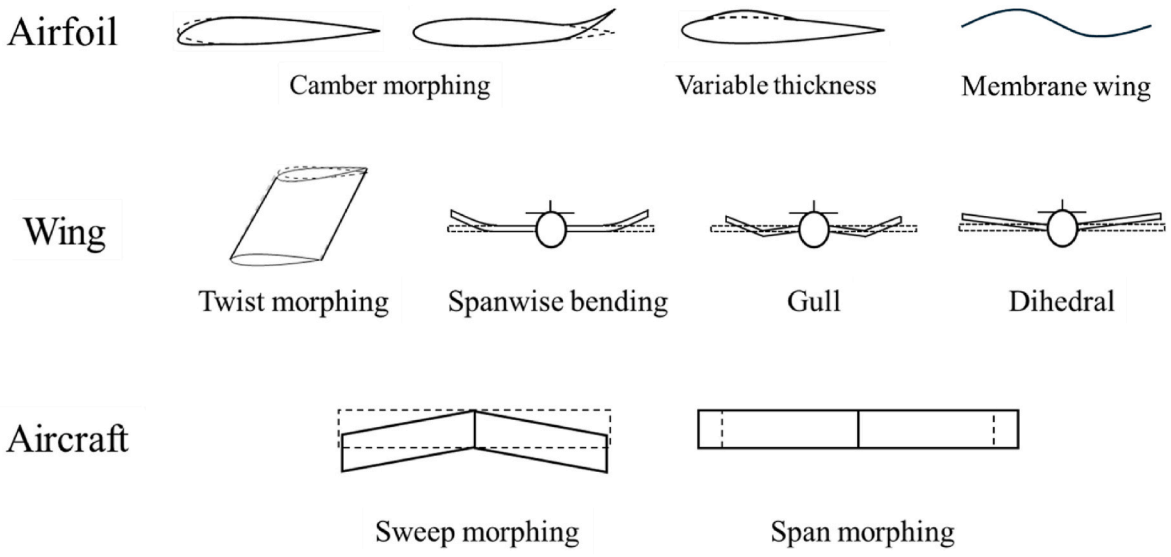

Fig. 1. Classification and schematics of morphing.

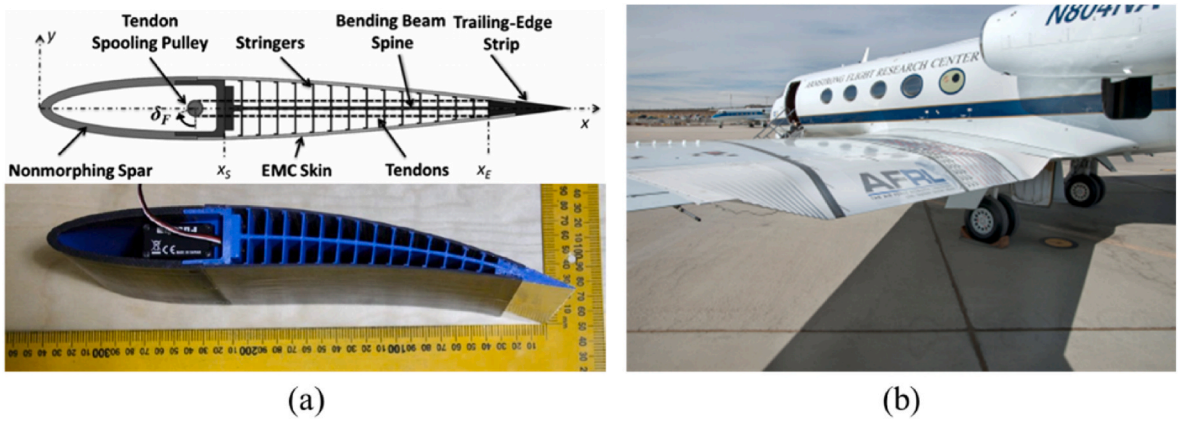

Fig. 2. Representative series of work of TE morphing: (a) FishBAC [9]; (b) ACTE [10].

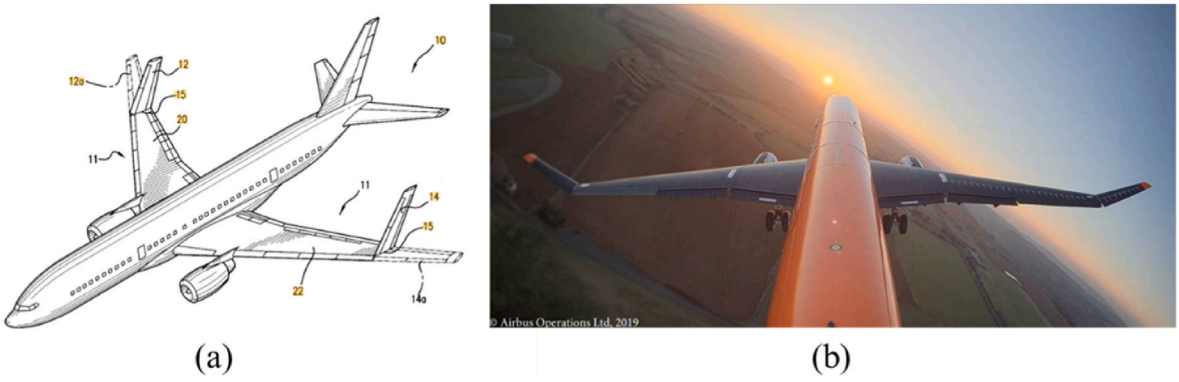

Fig. 3. Representative work of spanwise bending: (a) Boeing 777X [15]; (b) Albatross ONE [16].

control).

2.1. Leading and trailing edge morphing of airfoil

The benefits of steady aerodynamics, unsteady aerodynamics, and aeroelasticity are shown in Table 1. Due to the abundant investigation of camber morphing in aerodynamics, leading-edge (LE) and TE morphing have been demonstrated to significantly improve aerodynamic performance.

Compared to traditional hinged flaps, TE morphing significantly enhances lift-to-drag ratios under all lift coefficient ranges, especially the high lift coefficient range. LE morphing suppresses flow separation at the leading edge, which increases the lift peak and suppresses stall flutter. Furthermore, both LE and TE morphing affect flow separation and leading-edge vortex (LEV), which can be used to suppress stall flutter and alleviate gust loads.

As shown in Fig. 4, a bar chart presents the literature count on different morphing strategies and research objects to reflect the trend of related research. It is evident that TE morphing is the most popular morphing strategy in the airfoil planform.

Table 1
Aerodynamic and aeroelastic benefits of LE and TE morphing.

Morphing style	Steady aerodynamics	Unsteady aerodynamics	Aeroelasticity
LE morphing	**Increase lift** in subsonic flows [19–23] **Reduce Drag** [20,21,23] **Enhance lift-drag ratio** [20–23] Delay stall/suppress flow separation [22,24,25]	Prevent/control the formation of **LEV** [26,27] Reduce the **dynamic stall** effect/delay stall [26,28] **Enhance lift** through controlled flow separation [29] Improve power efficiency of flapping [30]	**Flutter**: Suppress stall flutter [27]
TE morphing	**Increase lift** in subsonic flows [19–21,31–34] **Reduce drag** [20,21,31,33–37] **Enhance lift-drag ratio** in subsonic flows [9,20,21,33,36,38,39] Delay stall/flow separation [20,31,33]	**Delay stall** [31,40] Improve averaged lift coefficient [28] and **lift-drag ratio** [34], decrease drag [31] Reduce reverse flow regions [41] Affect aerodynamic work due to pitch motion [30,42], improve power efficiency of flapping [30]	Improve **flutter** stability boundary/Eliminate stall flutter [43,44] Alleviate **gust** load [45–47]
Thickness	**Increase lift** in subsonic flows [48] **Reduce drag** in subsonic [48], transonic flows [49] **Enhance lift-drag ratio** in subsonic flow [48,50–52] Decrease noise [50]		

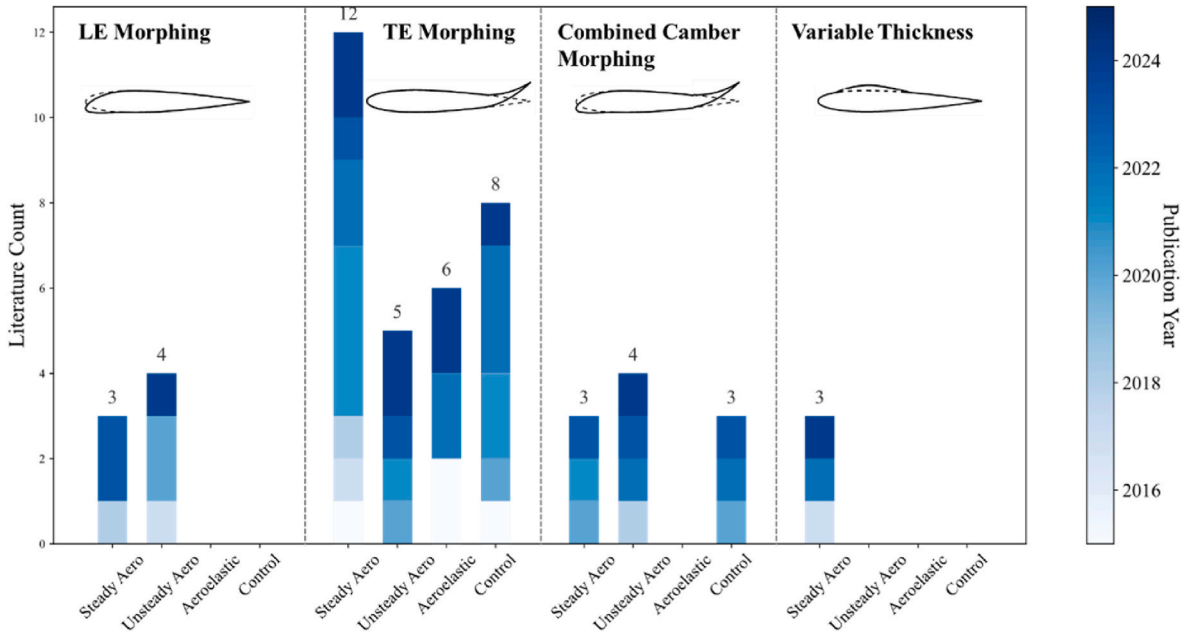

Fig. 4. Literature quantities and publication year at steady, unsteady aerodynamic, aeroelastic, and active control of LE, TE, combined morphing, and variable thickness.

In the past 10 years, the camber morphing has been continuously investigated, especially TE morphing. The research on variable thickness is relatively rare in unsteady aerodynamics and aeroelasticity. Therefore, this section mainly focuses on LE and TE morphing.

2.1.1. Steady aerodynamic characteristics

The steady aerodynamic effects of camber morphing wings have been extensively explored through diverse camber morphing strategies. Studies focusing on TE morphing dominate this field. **Nelson et al. (2024)** [31] demonstrated by a wind tunnel experiment that TE morphing alleviates the adverse effects of the reverse flow area on finite-span wings, including negative lift, drag increase, and large pitching moment impact. Similarly, **Wu et al. (2017)** [38] proposed a carbon-fiber composite airfoil with multi-degree-of-freedom TE morphing, achieving independent pitch moment control and high lift-to-drag ratios across a wide angle-of-attack range. **Dhileep et al. (2022)** [39] further validated the benefits of TE morphing via a Single Corrugated Variable-Camber (SCVC) structure, showing significant lift-to-drag ratio enhancements at moderate-to-high lift conditions.

In contrast, LE morphing has been optimized to delay stall applications. **Colletti and Ansell (2023)** [24] utilized genetic algorithms to design leading-edge geometries. The wind tunnel experiment was conducted to validate the suppression effect of LE morphing on flow separation at the leading edge. Similarly, **Magrini and Benini (2018)** [53] combined Class/shape transformation (CST) parameterization and genetic algorithms to optimize leading-edge shapes while maintaining constant arc length, ensuring compatibility with multiple aerodynamic models.

Combined leading-trailing edge morphing strategies have also emerged. **Nemati and Jahangirian (2020)** [19] proposed a robust parameter optimization framework for combined LE and TE morphing, achieving a 90% lift increase compared to cruise for a short period. **Wang et al. (2023)** [20] numerically demonstrated that smooth parabolic LE and TE morphing outperform hinged flaps for lift increase, drag reduction, and improved aerodynamic efficiency. LE morphing significantly delayed stall, TE morphing delayed flow separation, with aerodynamic efficiency further enhanced by higher aspect ratios in 3D wings.

These studies collectively emphasize the critical role of deformation components in tailoring steady aerodynamic performance, with TE morphing dominating aerodynamic efficiency improvements and flow separation suppression, and LE morphing addressing stall challenges.

The research on variable thickness morphing is relatively scarce. **Koreanschi et al. (2017)** [54] optimized the morphing parameters on the upper surface of the wing by genetic algorithms and validated the low speed drag reduction in wind tunnel experiments. **Magalhães et al. (2022, 2024)** [48,55] developed data-driven frameworks to predict the aerodynamic coefficient of variable-thickness airfoils. Based on the model, morphing shapes are optimized and extended to high-Reynolds-number flows.

Experimental validation of airfoil morphing is challenging to implement due to the realization of the morphing structure and control. However, there have been quite a few studies on experiments in recent years. **Chanzy and Keane (2018)** [35] conducted flight tests on a morphing UAV, showing a 40% drag reduction but a lower rolling rate than conventional flaps.

The Clean Sky Green Regional Aircraft (GRA) program, starting from 2006, aims at the green aeronautical technologies that best fit the European regional aircraft after 2025. Morphing and multifunctional wings for highly efficient aerodynamics are the critical technologies. As a progressive work, **Lin and Pecora et al. (2021, 2024)** [32,56] achieved industrial-scale success with TE morphing for large aircraft, demonstrating a 31.92% lift increase during takeoff and 9.04% during landing through wind tunnel tests, as shown in Fig. 5.

While experiments provide critical insights into real-world performance, numerical tools enable rapid exploration of complex morphing geometries and multi-objective optimizations. Numerical optimization is still the dominant investigation method of morphing. **Rana et al. (2022)** [57] optimized geometrical parameters of the morphing airfoil at Mach = 0.8, repositioning shock waves and significantly enhancing lift-to-drag ratios. **Magalhães et al. (2022, 2024)** [48,55] developed data-driven frameworks combining deep neural networks and meta-heuristic algorithms to predict the aerodynamic coefficient of morphing airfoils.

Different morphing design and manufacturing methods may also affect steady aerodynamic performance. Therefore, numerical simulations based on the morphing structures are conducted in some investigations, especially for some new materials and control methods. For

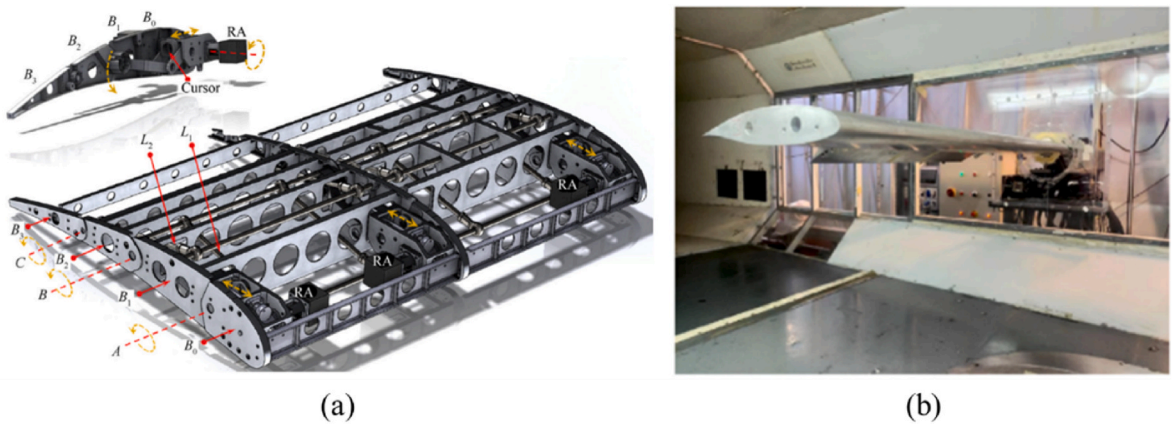

Fig. 5. Clean Sky GRA program: (a) morphing structure [32] and (b) wind tunnel test [56].

instance, **Zhang et al. (2021)** [36] integrated shape-memory alloys (SMAs) and macro-fiber composites (MFCs) into TE morphing. The numerical results demonstrated that the structure achieves active flow control and drag reduction. **Hao et al. (2021)** [33] designed a continuous TE morphing wing using multi-stable nanomaterials, showing improved lift-to-drag ratios at large AOAs and delayed flow separation in simulations. **Gu et al. (2021)** [21] combined topology optimization and SMAs to achieve precise shape control, validated aerodynamic performance through computational fluid dynamics (CFD). Advances in smart materials and structural optimization have enabled smoother, more reliable morphing mechanisms that are crucial for practical applications.

FishBAC, pioneered by **Woods et al. (2012–2021)** [6–9], is a typical example of TE morphing structure, as shown in Fig. 6. **Rivero et al. (2021)** [9] compared FishBAC morphing and conventional hinged flaps via wind tunnel experiments, proving at least 16% higher lift-to-drag ratios of FishBAC. **Fincham and Friswell (2015)** [37] demonstrated its aerodynamic superiority in multi-condition optimizations. **Clements and Djidjeli (2023)** [34] highlighted improved aerodynamic efficiency by FishBAC morphing and its effectiveness in ground effect.

Numerous studies on camber morphing have shown that it improves the lift-to-drag ratio and suppresses stall and flow separation. Besides, the numerical investigations of **Ortiz-Melendez et al. (2023)** [25] demonstrated that LE morphing of the airfoil delayed stall and increased maximum lift. Both LE and TE morphing make significant contributions to the steady aerodynamic performance.

2.1.2. *Unsteady aerodynamic characteristics*

The unsteady aerodynamic effects of camber morphing wings are closely tied to dynamic deformation strategies and their interaction with flow phenomena.

Studies on LE morphing highlight its role in suppressing dynamic stall and modulating vortex dynamics. For instance, **Ferrier et al. (2017)** [26] demonstrated that active LE morphing prevents the formation of LEVs and effectively reduces the dynamic stall effect. Similarly, **Kang et al. (2020)** [29] revealed that morphing LE skins at low Reynolds numbers significantly enhance lift through controlled flow separation when locked into the vortex shedding frequency. **Wen et al. (2024)** [27] further demonstrated LE morphing by introducing a 315° phase advance relative to pitching motion, which suppressed stall flutter and regulated LEV generation.

TE morphing has been explored for flow separation reduction, energy extraction, and flow stabilization. **Ko et al. (2021)** [41] demonstrated that passive TE morphing reduces reverse flow regions under both steady and unsteady conditions. **Wu et al. (2023)** [42] showed that TE morphing affects the LEV, changing the pressure distribution, as shown in Fig. 7(a). TE morphing at a phase offset of $-\pi/2$ reduced energy extraction by over 300% while mitigating stall-flutter limit-cycle oscillations. Similarly, **Kan et al. (2020)** [40] proposed periodic TE morphing to delay stall.

In the FishBAC project, **Clements and Djidjeli (2024)** [59] employed periodic FishBAC morphing in ground effect. The detached eddy simulation (DES) is adopted to resolve von Kármán vortices in wakes, linking vortex dynamics to lift enhancement.

Combined LE and TE morphing strategies amplify synergistic effects. **Hoke et al. (2023)** [30] reported a 36.2% efficiency improvement in energy extraction for flat plates using combined morphing. **Bashir et al. (2024)** [28] optimized morphing LE and morphing TE shapes, the

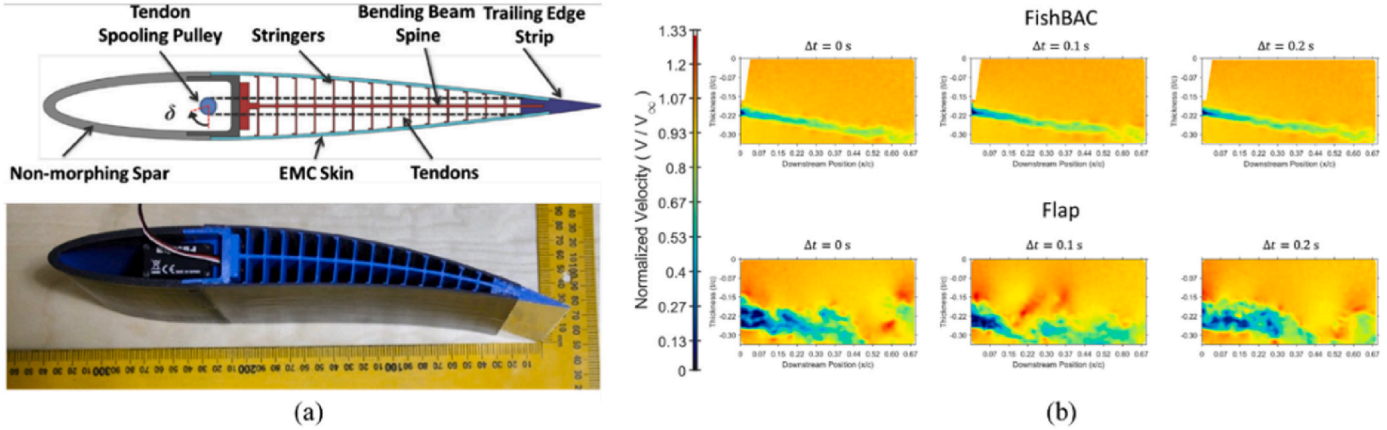

Fig. 6. FishBAC: (a) morphing structure [7] and (b) aerodynamic results [9].

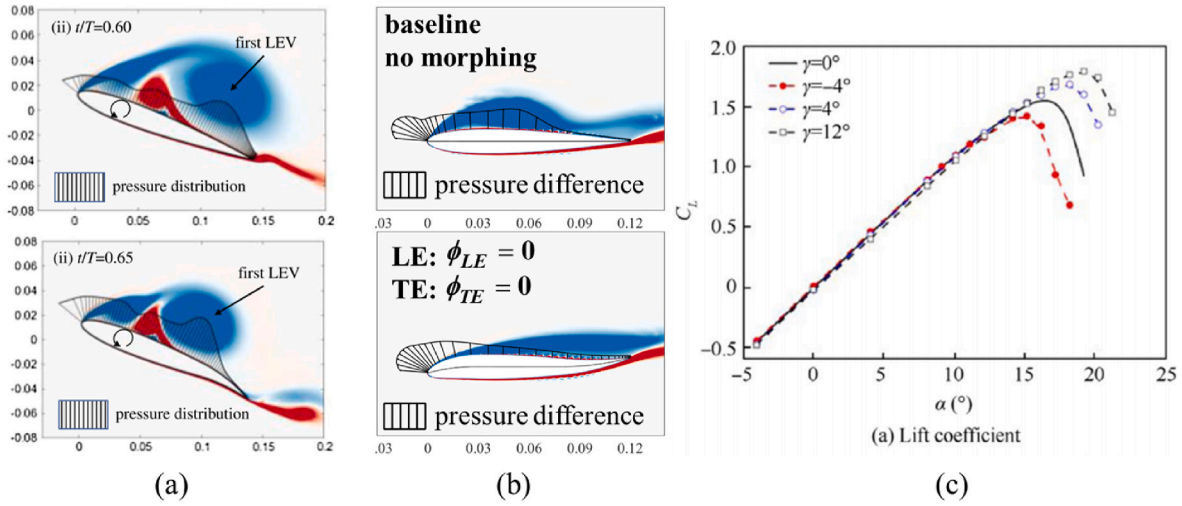

Fig. 7. (a) pressure distribution and vorticity of baseline and TE morphing of a pitching airfoil [42], (b)pressure distribution and vorticity of baseline and TE morphing of wing slice under gusts [58], and (c) lift coefficient of an airfoil with different LE morphing angles γ [22].

former delaying dynamic-stall AOA by 14.26% and the latter increasing the lift coefficients. **Dai et al. (2025)** [58] suppressed gust-induced LEV with combined LE and TE morphing and significantly alleviated gust loads, as shown in Fig. 7(b).

These studies underscore the tailored efficacy of deformation components: leading-edge morphing excels in vortex control, TE morphing stabilizes unsteady flows, and their combination unlocks synergistic performance gains.

Numerical modeling and linear aerodynamic models dominate unsteady aerodynamic research. **Fan and Breuer (2022)** [60] developed a 3D low-order model for flapping wings, integrating quasi-steady blade element momentum theory to quantify a 27% lift increase and 10% drag reduction from camber morphing. **Guo et al. (2024)** [61] employed CFD/CSD (computational structural method) coupling to analyze fluid-structure interactions in TE morphing, revealing how skin compliance, flow conditions, and actuation affect aerodynamic characteristics. **Li et al. (2018)** [62] derived an analytical unsteady lift model based on potential flow theory, simplifying the dynamic responses of camber morphing airfoils.

While numerical tools enable rapid exploration of complex morphing scenarios, experiments and high-fidelity simulations validate mechanisms and refine predictive accuracy. **Ko et al. (2021)** [41] adopted PIV measurements to investigate the passive TE morphing flow field in the wind tunnel experiments. **Kan et al. (2020)** [22] utilized the CFD method to obtain the unsteady aerodynamic characteristics of LE morphing, revealing the effect of LE morphing on dynamic stall, as shown in Fig. 7(c).

The interplay between morphing kinematics and vortex dynamics defines non-steady performance, with applications spanning stability control, energy harvesting, and flow separation management. A central focus lies in dynamic stall mitigation. **Bashir et al. (2024)** and **Ferrier et al. (2017)** [26,28] demonstrated that optimized LE morphing suppresses DSV formation and delays stall angles. **Kan et al. (2020)** [40] linked TE morphing rates to stall delay, while **Wen et al. (2024)** [27] emphasized phase-synchronized LE morphing to destabilize stall flutter.

Active TE morphing significantly impacts aerodynamic energy extraction, which can be adapted for flow stability analysis. Wu et al. (2023) [41] analyzed energy metrics to optimize TE motion for oscillation suppression. Aerodynamic energy extraction efficiency is also important for flapping wings. **Hoke et al. (2023)** [30] showed that combined morphing amplifies positive aerodynamic work and improves extraction efficiency during flapping.

Vortex control and lock-in mechanisms are critical for unsteady performance. **Kang et al. (2020)** [29] identified frequency locking between morphing actuation and vortex shedding as a key lift-enhancing mechanism.

2.1.3. *Aeroelastic modeling and characteristics*

Aeroelastic modeling of camber-morphing wings is a complex problem that requires simultaneous consideration of structure, aerodynamics, and camber-morphing factors.

Methodological advancements in aeroelastic modeling balance computational efficiency with fidelity. **Murugan et al. (2015)** [63] pioneered hierarchical modeling to decouple structural optimization from fluid-structure interaction (FSI), reducing computational costs without sacrificing critical physics. They decoupled compliant skin optimization from aeroelastic simulations, using homogenized beam models for efficient analysis. The study laid the groundwork for computationally affordable aeroelastic design. **Ochi et al. (2024)** [64] further emphasized experimental validation. They developed a loosely coupled finite element and hierarchical Cartesian grid solver to analyze the aeroelastic behavior of a passive TE morphing wing. The results have been validated through wind tunnel experiments, and it was revealed that the simulation results of RANS are more accurate than those of Euler.

Woods et al. (2015) [65] integrated a Euler-Bernoulli beam-based structural model with XFOIL aerodynamic simulations to predict equilibrium shapes, aerodynamic coefficients, and actuation requirements of FishBAC. The numerical model is validated by the experimental results, as shown in Fig. 8.

For active morphing systems, **Wright and Bilgen (2024)** [66] proposed a multi-objective optimization framework for piezoelectric composite-driven camber morphing airfoils, integrating XFoil for aerodynamic analysis and ANSYS for structural modeling. Their approach achieved static aeroelastic responses that maximized lift while minimizing deformation, demonstrating the feasibility of real-world deployment through prototype testing. **Hu et al. (2022)** [45] developed a fluid-structure interaction method of seamless wing morphing based on the CFD method and modal superposition method, considering the geometrical nonlinearity of the TE morphing.

Camber morphing also influenced the aeroelastic characteristics. **Syed et al. (2022)** [43] investigated the stability of a highly flexible flying-wing UAV and demonstrated that TE morphing significantly improved flutter stability, offering insights into long-endurance UAV design.

As a chordwise morphing strategy, the investigations on camber morphing are not yet thorough enough. In fact, the curvature of morphing can also change in the transverse direction, requiring

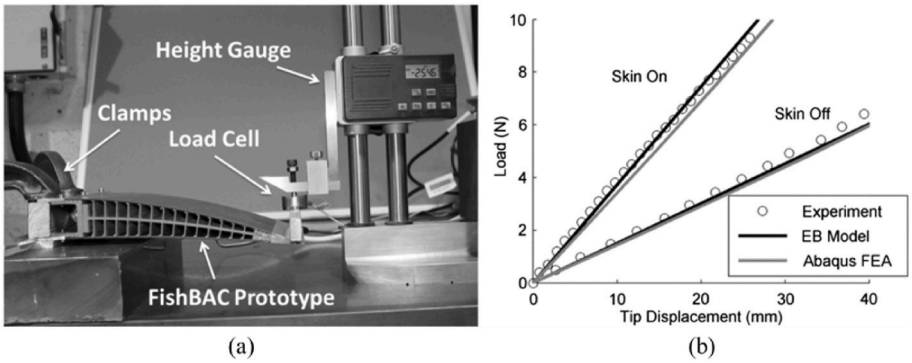

Fig. 8. FishBAC: (a) experiment model [65] and (b) validation results [65].

consideration in three-dimensional terms. The flow mechanism considering active wing morphing and passive elastic deformation also remains to be explored.

2.1.4. *Active control*

The control of camber morphing wings has evolved through sophisticated algorithms tailored to suppress aeroelastic instabilities and mitigate external disturbances. Nonlinear and dynamic inversion control stands out for camber morphing control. **Wang et al. (2022, 2021)** [46,47] proposed an incremental nonlinear dynamic inversion with quadratic programming control allocation and virtual shape functions (INDI-QP-V) for seamless morphing wings, reducing wing-root shear forces and bending moments by over 44% during simultaneous gust and maneuver load alleviation. The seamless wing and the alleviation results are shown in Fig. 9(c).

Li et al. (2024, 2025) [44,69] achieved complete stall-flutter elimination using a nonlinear-model-inversion (NMI) controller and a reinforcement learning trained controller, where TE morphing generated counteracting vortices to suppress stall flutter.

Time-delayed and feedback control strategies address real-world actuation constraints. **Wu et al. (2022)** [70] demonstrated that a proportional-derivative controller with a 0.1-s delay reduced stall-flutter limit-cycle amplitudes by 60%, leveraging CFD-based fluid-structure interaction (FSI) simulations to decode energy transfer

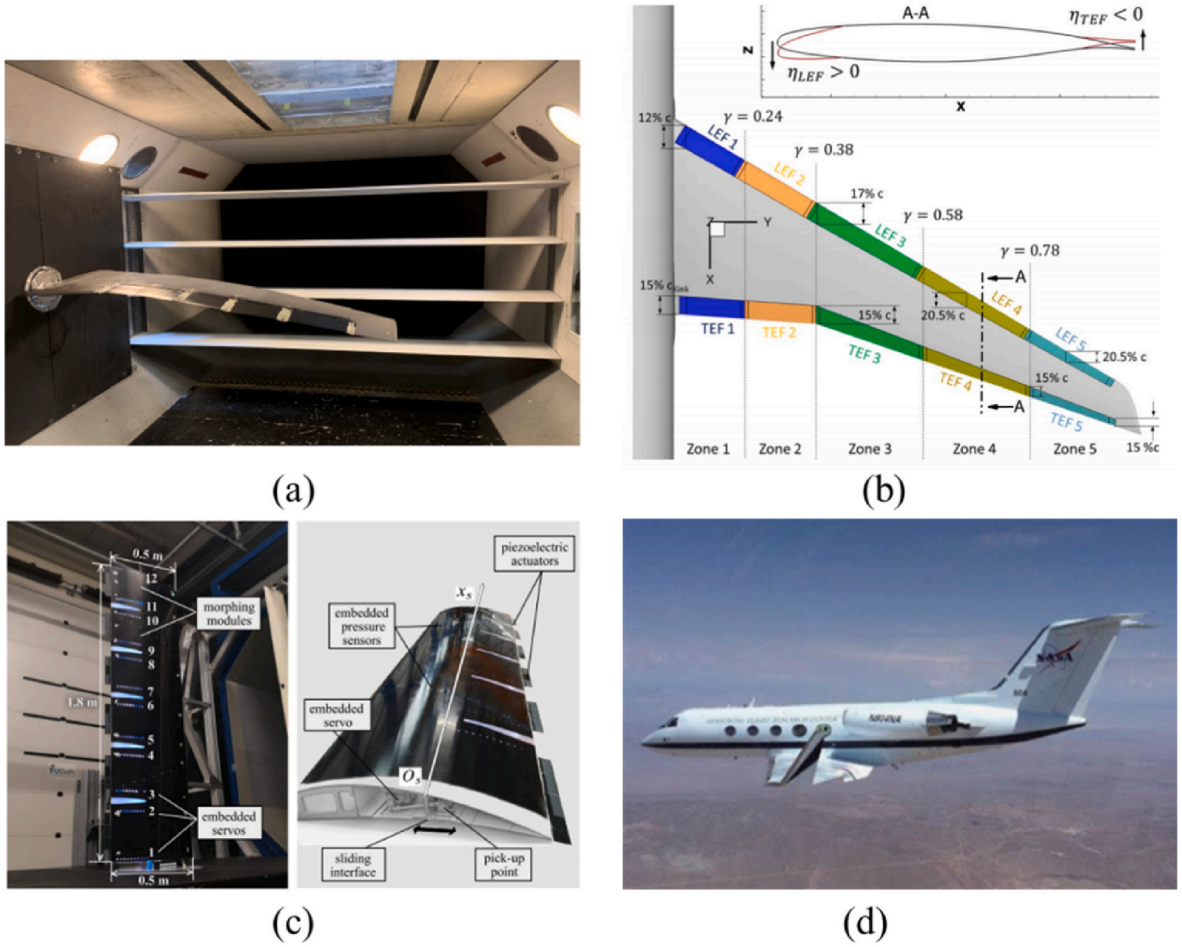

Fig. 9. (a) Wind tunnel experiment of VCCTEF [67], (b) spanwise-segmented TE and LE flaps [68], (c) seamless morphing wings [47], and (d) flight test of ACTE project [10].

mechanisms. **Zhang et al. (2021)** [71] proposed a morphing camber concept based on a continuous two-segment structure comprising a rigid segment and a deformable section. Their study examined the influence of key parameters, such as the length-to-chord ratio and stiffness of the morphing segment, on flutter behavior. To further stabilize the system, they incorporated feedback control into a FishBAC TE morphing device, effectively regulating pitch and plunge motions to mitigate aeroelastic instability.

These studies highlight the dominance of model-based control in handling nonlinearities, while time-delayed and feedback strategies bridge theoretical designs with practical actuation dynamics.

Camber morphing excels in gust load alleviation, both at transonic and low-speed conditions. **Ullah et al. (2022, 2023)** [68,72] employed spanwise-segmented TE and LE flaps, as shown in Fig. 9(b), showing that steady flap deflections reduced gust-induced wing bending moments by 54% and torsional moments by 58%. Dynamic flap deflections further achieved near-complete load cancellation. In the same team, **Klug et al. (2020)** [73] highlighted TE flaps' superiority, compensating for 95% of gust-induced lift perturbations at moderate AOA. In the variable camber continuous trailing edge flap (VCCTEF) system by **Nguyen and Berg et al. (2020)** [67,74], the GLA for a camber morphing wing is investigated by numerical methods and experiments, as shown in Fig. 9(a).

While segmented flaps excel in localized load redistribution, seamless morphing enables holistic aerodynamic adaptation, balancing aerodynamic efficiency and control ability. **Hu et al. (2022)** [45] implemented a time-domain feedforward control based on seamless wing morphing, achieving a 10%-53% reduction under different gust amplitudes. **Wang et al. (2021, 2022)** [46,47] extended the conventional GLA by combining seamless morphing with INDI-QP-V, demonstrating simultaneous gust and maneuver load reduction in wind tunnel tests. The ACTE project [10] has conducted a flight test of the seamless morphing wing, as shown in Fig. 9(d). A flight of Mach 0.85 was achieved on a modified Gulfstream III aircraft equipped with a three-dimensional seamless TE morphing with the maximum morphing angle of 10°.

TE dominance is evident in both flutter suppression and gust control. **Li et al. (2024, 2025)** and **Wu et al. (2022)** [44,69,70] linked trailing edge vortices (TEV) to flutter destabilization, while **Ullah et al. (2023)** [72] optimized TE flaps for transonic gust alleviation. In contrast, leading-edge contributions are niche but impactful. **Klug et al. (2020)** [73] found that TE flaps mitigated 50% of nose-up pitching moments without significantly altering lift responses, underscoring their role in moment equilibrium. TE actuation remains the cornerstone of morphing control, but hybrid strategies incorporating leading-edge and seamless deformation are emerging as versatile solutions. It is worth mentioning that, in earlier studies, the use of combined LE and TE control surfaces has also been proposed to mitigate control surface reversal in flexible wings [75,76].

The active control work mainly adopts TE morphing. The abundant research shows that TE morphing can basically replace the conventional control surfaces and serve as one of the control surfaces for future aircraft. While LE morphing has a relatively small contribution to aerodynamics, it plays a significant role in aerodynamic moments and the formation of leading-edge vortices. It also has considerable potential for active control.

2.2. Twist and spanwise morphing of wing

Table 2 summarizes the aerodynamic and aeroelastic benefits of four types of wing morphing. Sufficient research shows that spanwise bending can improve the flutter boundary and alleviate gust loads. Twist morphing significantly improves steady aerodynamic performance.

The literature count and publication years of this chapter are shown in Fig. 10. Active control via spanwise morphing is popular in recent years, especially aeroelastic control. Regarding the spanwise morphing, the focus in the early stage is on aeroelastic characteristics. However, in recent years, the research on its application in control is significantly increasing.

The research on gull and dehidral are relatively scarce, especially in aeroelasticity. This section mainly focuses on studies of spanwise morphing. In each section, four morphing strategies are introduced in sequence.

2.2.1. Steady aerodynamic characteristics

2.2.1.1. Twist morphing. Twist morphing has demonstrated significant potential in enhancing steady-state aerodynamic performance across various aircraft configurations. **Kaygan and Ulusoy (2018)** [77] employed the Athena Vortex Lattice Method (AVLM) to analyze twist angles ranging from −8° to 8° on an Airbus A320 wing model. Their results revealed that optimized twist distributions could improve lift-to-drag ratios at low angles of attack, validating twist morphing as a viable strategy for flight control. As shown in Fig. 11, **Rodrigue et al. (2016)** [78] conducted wind tunnel tests on a UAV wing with segmented twist deformation, showing almost a 13% increase in lift-to-drag ratio at 2° angle of attack and a maximum lift coefficient improvement at 8° angle of attack.

For the flying wing, **Kelayeh and Djavareshkian (2021)** [99] performed CFD simulations on a uniformly twisted flying wing, identifying a "neutral brink angle" beyond which twist effects diminished. While aerodynamic efficiency improved at high angles of attack, performance degraded at 0° angle of attack as the twist angle increased.

Jasa et al. (2018) [79] integrated gradient-based optimization for a morphing wing, combining twist and altitude profile adjustments. Their approach reduced fuel consumption by 0.2–0.7%, with surrogate models achieving optimization accuracy within 1.5% of fully coupled methods.

2.2.1.2. Spanwise bending. Spanwise bending morphing, particularly through foldable wingtips, has demonstrated significant potential in enhancing steady-state aerodynamic performance. **Cooper et al. (2015)** [85]pioneered the design of flexible folding wingtips using CFD and neural network surrogate models. Their approach reduced abrupt flow-induced loads by 5% and fuel consumption by 3% for reference missions, validating the lightweight potential of morphing wingtips.

Table 2
Aerodynamic and aeroelastic benefits of twist, spanwise morphing, gull, and dihedral.

Morphing style	Steady aerodynamics	Unsteady aerodynamics	Aeroelasticity
Twist morphing	**Improve lift-to-drag ratio** at low AOAs [77,78] Fuel consumption reduction [79] Smooth post-stall lift curve [80–83]	-	**Gust** load alleviation [84]
Spanwise bending	Fuel consumption reductions [85] **Drag reduction** [86]	-	**Flutter** boundary improvement [87] **Gust** load alleviation [88–91]
Gull	-	Enhance lateral maneuverability [92] Improve aerodynamic efficiency [93]	-
Dihedral	Complex effect on lift-to-drag ratio [94,95] Alter lateral and directional stability [94–96]	**Improve lift** at high AOAs [97] Improve energy efficiency [98] Reduce wind gradient requirements for soaring [98]	-

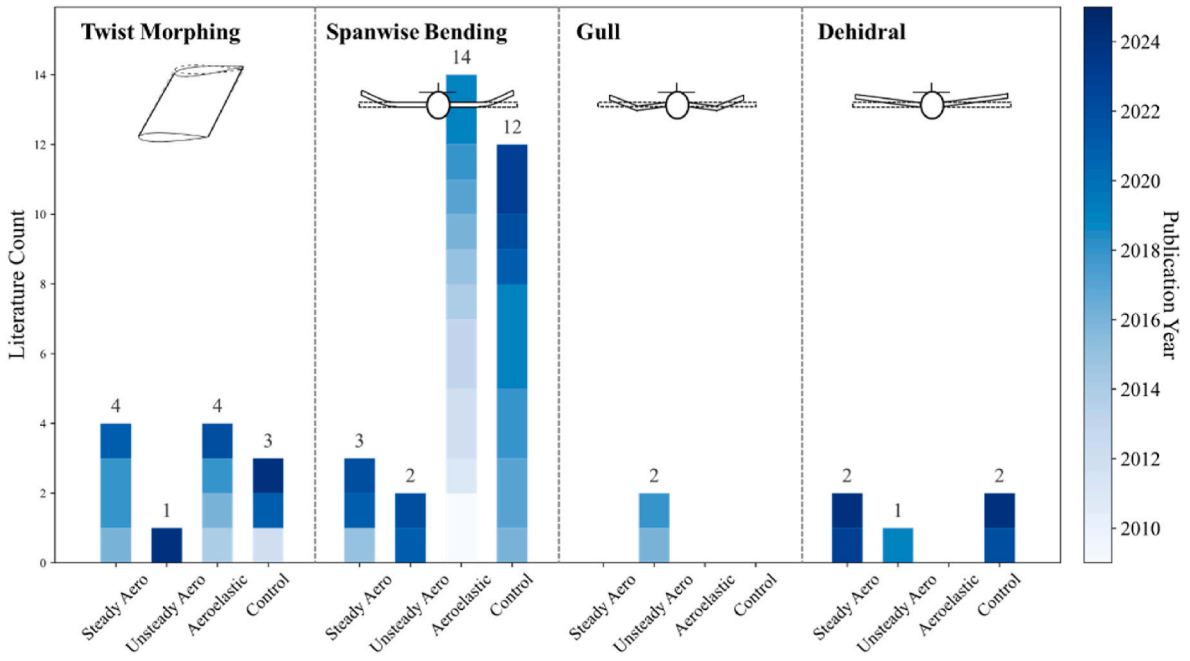

Fig. 10. Literature quantities and publication year at steady, unsteady aerodynamic, aeroelastic, and active control of twist, spanwise morphing, gull, and dihedral.

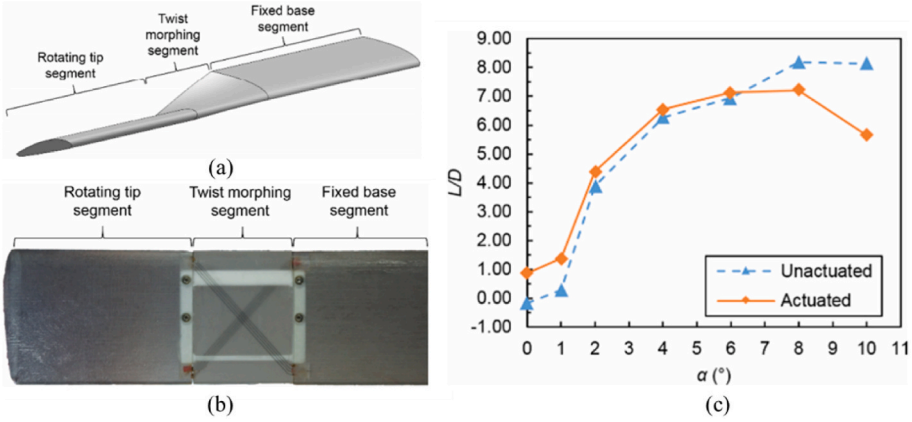

Fig. 11. (a)Morphing shape [78], (b)Complete morphing wing assembly [78], and (c)lift-to-drag ratios of twist morphing wing and baseline [78].

Kazim et al. (2022) [100] optimized variable-geometry winglets for the ONERA M6 airfoil, identifying a configuration with a 30° cant angle and 65° sweep that improved lift-to-drag ratios by 5.33%, with outward-canted angles enhancing flow attachment. Complementing these findings, **Eguea et al. (2021)** [86] employed a mid-fidelity method coupled with Fluent CFX to study camber-morphing winglets. Their results showed a significant reduction in induced drag due to weakened tip vortices.

2.2.1.3. Dihedral morphing. **Chang et al. (2023, 2024)** [94,95] established an aerodynamic model with a uniform experimental design method, CFD, and kriging algorithm. The wing configurations with wing dihedral are shown in Fig. 12. Under hypersonic conditions, L/D is highly sensitive to positive dihedral angles: small angles of attack see sharp L/D reduction with dihedral increase, while anhedral angles cause a brief rise followed by a gradual decline. At high angles, dihedral effects diminish. Under subsonic conditions, L/D responds more strongly to dihedral changes at low angles, with anhedral delaying L/D drop at low angles.

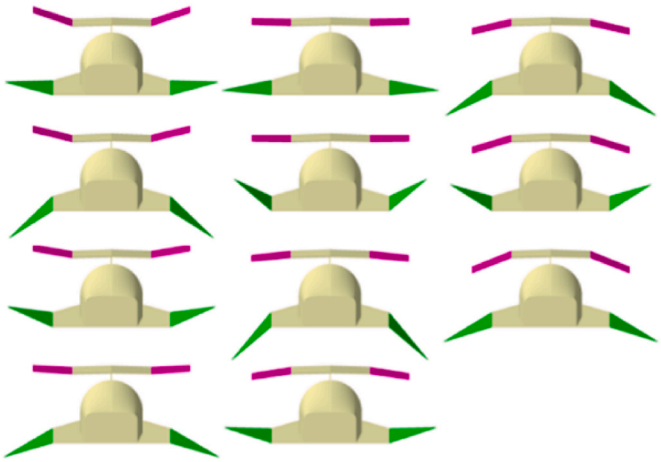

Fig. 12. Wing configuration with wing dihedral [94].

2.2.2. Unsteady aerodynamic characteristics

2.2.2.1. Twist morphing. Dynamic responses of twist morphing under unsteady conditions remain underexplored but critical for practical applications. **Karimi Kelayeh and Djavareshkian (2024)** [101] proposed co-directional and counter-directional twist control strategies for a highly swept flying wing. The CFD analysis demonstrated efficient pitch and roll moment generation at low angles of attack. To address unintended yaw moments during roll maneuvers, they introduced a composite twist arrangement.

2.2.2.2. Spanwise bending. To date, limited research has been conducted on the unsteady aerodynamic characteristics of spanwise bending. **Joshi and Bhattacharya (2022)** [102] conducted towing tank experiments on a flat plate with controlled spanwise bending at a 90° angle of attack to imitate a wing during a dive maneuver. The study revealed that bending toward the flow increased unsteady drag, while reverse bending suppressed initial force peaks, with vortex interactions dominating transient responses. **Jia et al. (2021)** [103] executed Direct Numerical Simulations (DNS) and experiments on a 30° swept wing, demonstrating that dynamic bending delayed LEV growth at 80% spanwise locations. **Dai et al.** [104] analyzes how morphing frequency and amplitude affect the unsteady force characteristics and performance of a spanwise-morphing wingtip, proposes a scaling law based on a generalized Duffing–van-der-Pol model, and reveals the dominant role of morphing amplitude in shaping force-response phase, harmonic content, and vortex-structure topology.

Spanwise morphing is often accompanied by complex three-dimensional flow, yet current studies on the underlying flow mechanisms remain relatively limited, and none have taken structural coupling into account.

2.2.2.3. Gull morphing. **Guo et al. (2016)** [92] developed a nonlinear flight dynamics model for a gull-morphing wing, considering the change of center of mass and inertia. The analysis revealed that asymmetric morphing significantly enhances lateral maneuverability but induces roll and slip motions, while symmetric morphing changes the balance point of the aircraft. **Harvey (2018)** [93] conducted wind tunnel tests on gull-wing configurations with folding angles ranging from 90° to 154°, mimicking seabird gliding postures. Lower elbow angles improved aerodynamic efficiency but reduced passive pitch stability.

2.2.2.4. Dihedral morphing. **Roy et al. (2019)** [97] explored the effects of dihedral and anhedral angles on a double-delta wing at low speeds. The wind tunnel and simulation analyses revealed that small anhedral angles improve lift at high angles of attack by shifting vortices inward.

2.2.3. Aeroelastic modeling and characteristics

2.2.3.1. Twist morphing. Aeroelastic interactions in twist morphing systems have been systematically investigated for micro aerial vehicles (MAVs). The **Ismail et al. (2014–2022)**[80–83]combined FSI simulations and wind tunnel tests to evaluate wash-in and wash-out twist configurations. The morphing shapes are shown in Fig. 13. Wash-in deformation increases lift-to-drag ratios but raises drag due to stronger wingtip vortices. The smooth post-stall lift curve of the wash-in configuration enhances the maneuverability of MAVs, which improves indoor missions and obstacle avoidance flights. Conversely, wash-out configurations exhibit weaker vortices, marginally reducing drag but failing to offset lift losses.

2.2.3.2. Spanwise bending. Aeroelastic interactions in spanwise bending systems have been a focal point in the last decades. **De Breuker et al. (2011)** [105] integrated nonlinear aeroelastic effects into folding wingtip design, combining beam models with Weissinger's aerodynamic theory. The optimized winglets reduced energy consumption by almost half compared to fixed configurations.

Despite the superior aerodynamic performance of folding wingtips, their aeroelastic stability is a significant challenge in practical applications. **Hu et al. (2016)** [106] numerically investigated the aeroelastic stability of a folding wing and proposed a stability criterion. As shown in Fig. 14, **Wilson et al. (2017)** [107] explored hinged wingtips through engineering models and wind tunnel tests, identifying hinge stiffness and damping as critical factors for flutter suppression. The **Ni and Zhao series (2015–2019)** [108,109] investigated folding wings utilizing nonlinear aeroelastic models and component modal synthesis methods. Their work revealed that nonlinear effects, such as hinge location and stiffness, dominated aeroelastic stability at high dynamic deformation rates.

The dynamic response and transient analysis of spanwise bending have also been investigated, especially flutter analysis. **Snyder et al. (2009)** [110] investigated the flutter characteristics of a folding wing through linear elastic beam and strip theories. The results indicate that flutter frequency decreases with increasing folding angle. **Zhao and Hu (2012–2013)** [111,112] established parameterized aeroelastic models to predict transient responses and analyze flutter characteristics. It is revealed that the flutter characteristics are significantly affected by folding angles. **Jung et al. (2013)** [113] demonstrated that optimal folding angles improve flutter boundaries by 20%.

To present the effects of each parameter of the folding wingtip more intuitively, the following Table 3 has been summarized.

Besides the investigations on aeroelastic characteristics, the advanced simulation frameworks are proposed. **Verstraete et al. (2019)** [115] proposed a CFD-FE coupling simulation methodology to simulate nonlinear aeroelastic behavior across flight conditions. **Liska**

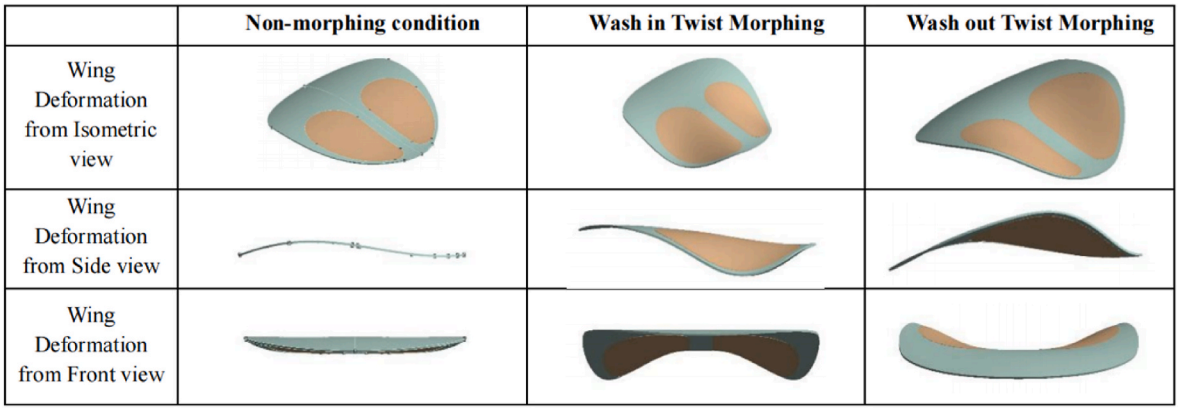

Fig. 13. Wash out and wash in twist morphing on MAV wing [83].

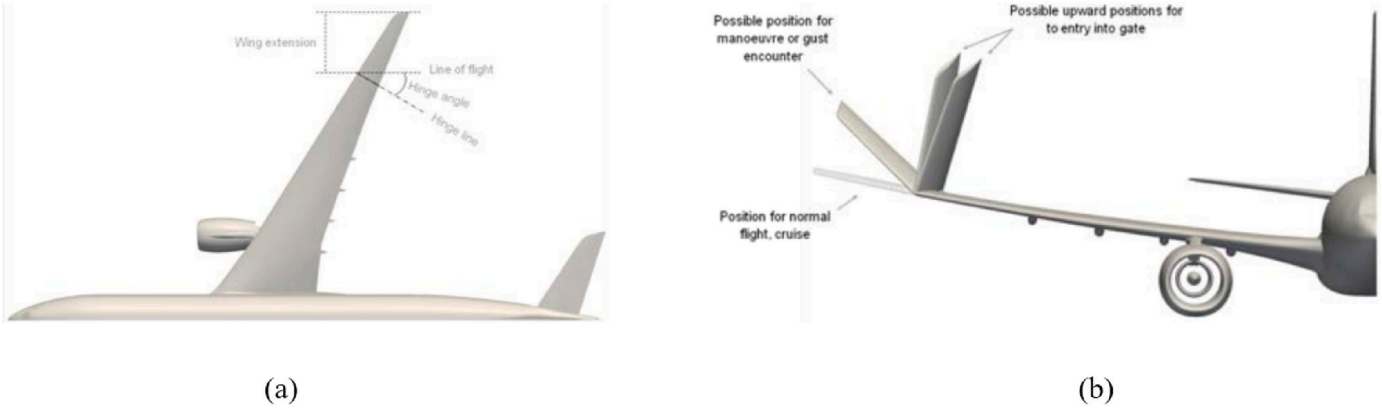

Fig. 14. (a) Folding wing tip for loads alleviation concept [107], (b) Front view of the concept showing various positions of the fold in different situations [107].

Table 3
effect of parameters of the folding wingtip on aeroelastic characteristics.

Parameters	Influence
Mass	A low wing-tip mass was beneficial for the aeroelastic stability both for flexible and fixed hinges [90].
Flare angle	Flare angle brings a better gust mitigation effect [84,89,90].
Wingtip length	A longer wingtip length brings a better gust mitigation effect [84].
Hinge damping	A nonzero hinge damping value was beneficial, allowing there duction of the inertial load [88]
spring stiffness	A smaller spring stiffness corresponds to a better gust mitigation effect [84,89,114].

et al. (2009) [116] developed unsteady potential flow theory with modal approaches for continuum aeroelastic modeling.

Multi-segment folding wings and Z-shaped wings exhibit significant improvement in aerodynamic performance, while the deteriorative stability and aeroelastic characteristics have become obstacles to their application. **Wang et al. (2012)** [117]investigated multi-segment folding wings using substructure and panel methods, showing a 15% lift-to-drag ratio improvement but a 10% reduction in flutter speed. **Mardanpour et al. (2014)** [87] analyzed Z-shaped passive morphing wings, as shown in Fig. 15, achieving 10–15% improvement on lift-to-drag ratio at the cost of stability degradation at high speeds.

In aeroelastic modeling and characteristic analysis, structural nonlinearities induced by large deformations are accounted for in various ways, whereas aerodynamic nonlinearities are seldom considered. For gull and dihedral morphing, current research focuses on aerodynamic performance, leaving a gap in aeroelastic coupling analysis.

2.2.4. Active control

2.2.4.1. Twist morphing. Active control strategies leveraging twist morphing have shown promise in replacing conventional control surfaces. **Pecora et al. (2012)** [118] developed an aeroelastic model comparing aileron-based and twist-based roll control for high-aspect-ratio wings. The results indicate that spanwise-linear twist distributions achieved 1.6 times higher roll rates than ailerons, requiring only minor twist angles for equivalent control authority. **Lobo do Vale et al. (2021)** [119] demonstrated limited roll control capability but significant load alleviation potential of a coupled twist-camber morphing wing through lift line theory. Flight tests exhibit roll control potential in no-wind conditions, while the energy consumption and structural weight are still to be considered.

Ahmadi et al. (2024) [84] analyzed passive twist-fold wingtips using mid-fidelity aeroelastic models, showing that twist morphing significantly reduced root bending moments, while folding configurations better suppressed flutter. However, low hinge stiffness exacerbated flutter risks, particularly near the leading edge.

2.2.4.2. Spanwise bending. Active control strategies for spanwise bending morphing have evolved from theoretical models to validated prototypes. The research team led by **J.E. Cooper** [88–90,114,120–122] et al. has pioneered innovative studies on foldable wingtip systems, focusing on gust load alleviation, aeroelastic stability, and flight dynamics integration. Their work spans conceptual design, wind tunnel validation, and nonlinear control optimization, offering transformative solutions for next-generation adaptive wing technologies.

In early explorations, the folding wingtip is adopted for gust load alleviation. **Castrichini et al. (2016)** [88] initiated research by investigating nonlinear folding wingtips for commercial jet applications. Using vortex lattice methods (VLM) in LMS Virtual.Lab, they

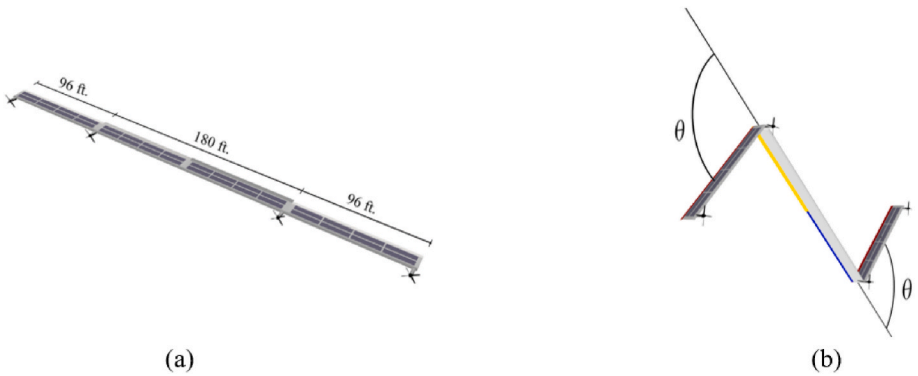

Fig. 15. (a)Geometry of the flying wing [87] and (b) schematic front view of the morphed configuration of the flying wing [87].

demonstrated that passive folding mechanisms could reduce root bending moments by 18–22% under moderate-to-high frequency gusts. A follow-up study (**Castrichini et al., 2017**) [89] introduced negative-stiffness springs, which reduced transient bending moments by 25%, particularly effective in high-frequency gusts. These studies highlighted the critical role of hinge damping and stiffness thresholds in load alleviation.

Then the research focus shifted to the hinge design and aerodynamic optimization. Building on previous findings, **Castrichini et al. (2017)** [90] further explored hinge configurations, revealing that hinges aligned at 25° to the free-stream direction with low stiffness could alleviate up to 30% of static and dynamic loads. Concurrently, **Cheung et al. (2018)** [114] conducted pioneering wind tunnel investigations on three hinged wingtip configurations (stiffness-hinge, free-hinge, and sprung-hinge) for gust load alleviation. Experimental data demonstrated that free-hinge arrangement achieved 56% peak rolling moment reduction during transient gusts, surpassing spring-loaded counterparts in dynamic response mitigation.

Based on the above research, an active folding wingtip was applied to gust load alleviation, and the flight dynamics of the active wingtip were analyzed. The team transitioned to active control strategies in **Wilson et al. (2019)** [120], patenting a semi-aeroelastic hinge device. This feedback-controlled system dynamically adjusted wingtip angles in real time, reducing peak gust loads by 30% and improving structural efficiency and life. A subsequent study (**Cheung et al., 2019**) [121] extended this work to high-aspect-ratio wings under 1-cos gust conditions, as shown in Fig. 16. The movable secondary aerodynamic surface on the folding wingtip stables the wingtip orientation across tested speeds and angles. The folding wingtip controller by the secondary aerodynamic surface enabled an 11% load reduction in long-duration gusts. **Castrichini et al. (2019)** [122] addressed flight dynamics coupling effects, confirming that folding wingtips did not compromise handling qualities.

The research on spanwise bending conducted by other teams has also contributed to the control of folding wings. **Fonte et al. (2018)** [123] implemented feedforward control on regional aircraft with morphing winglets, reducing wing-root and wingtip bending moments by 2.5% and 82.6%, respectively. **Ajaj (2021)** [124] highlighted the negative impact of structural flexibility on folding effectiveness, noting that increasing flare angle mitigated adverse effects on roll rates and aileron efficiency. **Balatti et al. (2022–2023)** [91,125] optimized wingtip parameters using genetic algorithms and used PD controllers for GLA. Introducing springs between the wingtip and the wing or reducing the flare angle can increase flutter speed without significantly affecting GLA. **Yao et al. (2023)** [126] conducted wind tunnel experiments for the spanwise morphing wing to investigate the effect of amplitude and frequency on gust alleviation.

Control research on spanwise morphing has focused on passive control and rudimentary active control, with a notable lack of studies on intelligent active control of the wingtip; additionally, aerodynamic nonlinearities have rarely been considered. According to gull morphing, existing work emphasizes passive morphing, with no implementation of real-time control.

2.2.4.3. Dihedral morphing. Recent studies on dihedral and anhedral wing configurations have demonstrated their significant impact on aircraft stability across varying flight regimes. **Meng et al. (2025)** and **Liu et al. (2022)** [96,127] investigated double-swept wave riders, focusing on low-speed and hypersonic conditions, respectively. Both

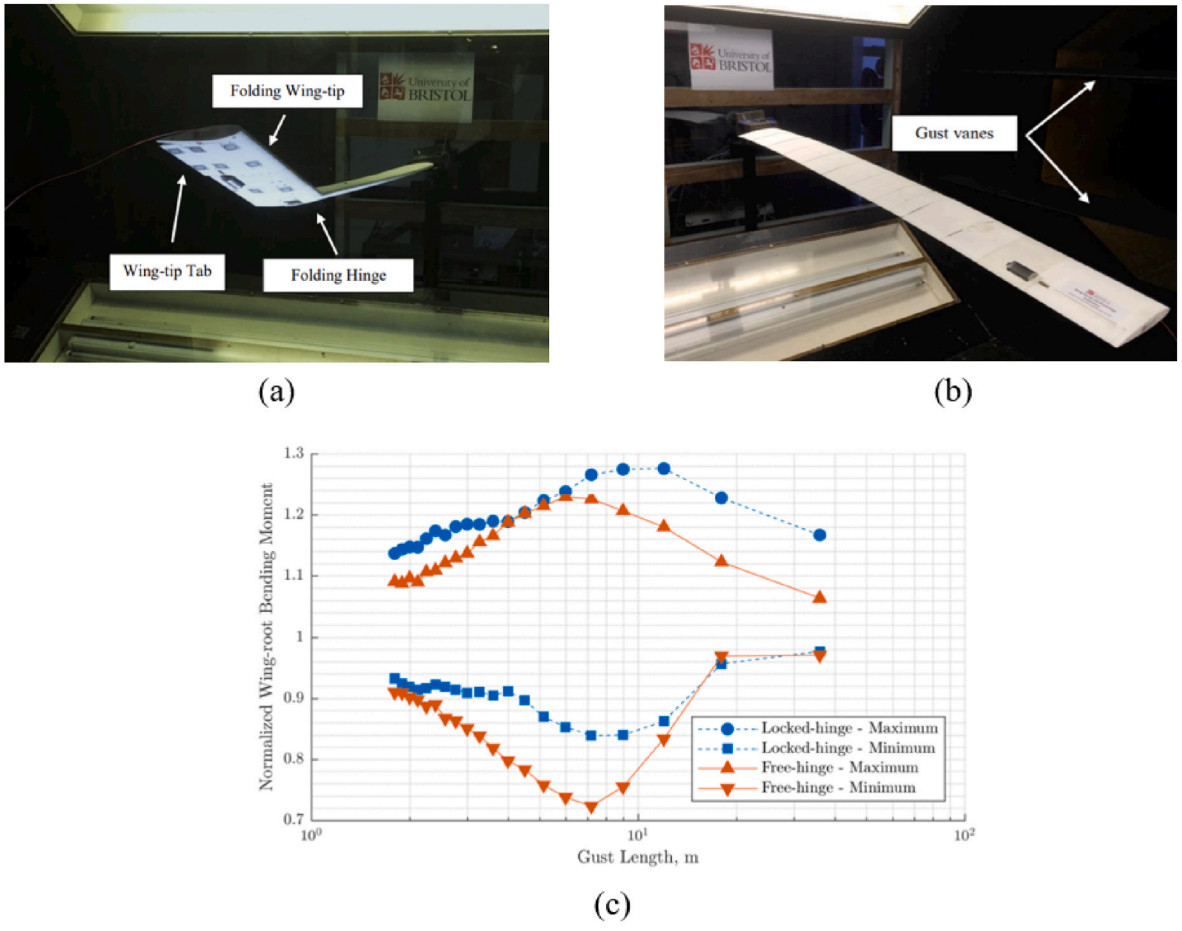

Fig. 16. (a) Wind model [121], (b) Model in the wing tunnel [121] (c) Load envelope of wing-root bending moment [121].

studies highlighted that dihedral angles barely affect lift-to-drag ratios but significantly alter stability. Wing dihedral improved lateral and directional stability, while wing anhedral reduced lateral stability.

The investigation of **Chang et al. (2023, 2024)** [128,129] also drew conclusions about stability. Under hypersonic conditions, longitudinal stability is weakly influenced by dihedral angles, while anhedral angles significantly enhance directional stability. Dihedral improves lateral stability while anhedral reduces it. Under subsonic conditions, dihedral angles of the delta wing offer greater overall advantages in improving stability characteristics of this configuration.

The study on active control by variable-dihedral wings is lacking. **Zhang et al. (2024)** [98] introduced a bio-inspired variable-dihedral wing for unmanned aerial vehicles. Their dynamic soaring optimization showed that a morphing anhedral wing (5°–50°) outperformed fixed configurations, improving energy efficiency by 2.52%-25.43% and reducing wind gradient requirements by 2.07%-15.56%. This innovative approach bridges static dihedral studies with adaptive designs, highlighting future directions for morphing wing technologies.

2.3. Sweep and span morphing of aircraft planform

The aerodynamic and aeroelastic benefits of sweep and span morphing are shown in Table 4. The aircraft's configuration change contributes to the flutter suppression and adaptability in different flight conditions. Both two morphing strategies have a significant impact on the configuration change and are relatively difficult to achieve.

The literature quantities and publication year of sweep and span morphing are shown in Fig. 17. Although they were proposed a long time ago, relatively few studies have been conducted in recent years.

The aeroelastic characteristics of sweep morphing have gradually attracted attention in recent years. There have also been new studies on span morphing.

2.3.1. Steady aerodynamic characteristics

2.3.1.1. Sweep morphing. Sweep morphing suppresses flow separation and optimizes vortex dynamics, enabling efficient multi-mission adaptability. **Zhang et al. (2020)** [137] employed DNS to analyze laminar separation over swept wings, revealing that midspan effect and large sweep angles stabilize wake flow via streamwise vortical structures. Building on this, **Ribeiro et al. (2022, 2023)** [138,139] conducted a series of DNS and resolvent analyses, demonstrating that sweep angles alter vortex shedding patterns and affect flow separation. They provided new insights into the mechanism of flow instability and flow control strategies.

Sweep morphing has proven effective in optimizing steady aerodynamic performance across multiple flight regimes. **Elelwi et al. (2020)** [140] combined XFLR5 and ANSYS Fluent to study tapered wings with variable sweep, achieving a 32.93% improvement in aerodynamic efficiency. **Dai et al. (2020)** [130] extended this concept to a morphing waverider, as shown in Fig. 18, validating its adaptability of four sweep configurations across subsonic to hypersonic speeds. The studies collectively highlight sweep morphing's capability to enhance flow stability and multi-speed performance.

Table 4
Aerodynamic and aeroelastic benefits of sweep and span morphing.

Morphing style	Steady aerodynamic	Unsteady aerodynamic	Aeroelastic
Sweep morphing	Enhance multi-speed domain adaptability [130]	**Increase time-averaged lift** [131]	Increase **flutter** speed [132]
Span morphing	**Improve lift-to-drag ratios** [133] Increase flight endurance and range [133]	-	**Flutter** suppression [134–136]

2.3.1.2. Span morphing. Span morphing significantly enhances steady aerodynamic performance and improves flight endurance by increasing span length. **Si et al. (2024)** [133] validated these findings through CFD simulations and flight tests on a foldable span-extendable UAV, reporting a 36.94% increase in lift-to-drag ratio and an 86.22% improvement in flight endurance. The study underscores the potential of span morphing for long-endurance missions.

2.3.2. Unsteady aerodynamic characteristics

2.3.2.1. Sweep morphing. Dynamic sweep morphing introduces complex unsteady effects, while dynamic hysteresis remains a critical challenge for real-time control. **Han et al. (2014)** [141] numerically investigated UAVs with variable-sweep wingtips, revealing the effect of flow hysteresis and added velocity. **Wang et al. (2022)** [142] integrated bio-inspired flapping with local sweep morphing, boosting lift coefficients, maneuverability and stability. Similarly, as shown in Fig. 19, **Zeng et al. (2023)** [143] used overset grids to analyze hysteresis mechanisms, emphasizing the effects of additional velocity, flow hysteresis and air viscosity. **Bai et al. (2025)** [144] developed an unsteady vortex-lattice model for shear variable-swept wings, showing that increasing sweep angles reduce lift-to-drag coefficients and induce clockwise hysteresis loops. **Xi et al. (2025)** [145] numerically investigated the aerodynamic forces and flow field of a shear-variable sweep wing at low Reynolds numbers, highlighting distinct wake characteristics across different reduced frequencies.

2.3.2.2. Span morphing. Research on the unsteady aerodynamic characteristics of a variable-span wing is still relatively scarce. **Si et al. (2024)** [146] investigated transient aerodynamics in tube-launched UAVs, revealing that the transient aerodynamic force creates a dynamic hysteresis loop around the quasi-steady data. It is attributed to the hysteresis effect of flow, and the force distribution is changed by influencing the formation of wingtip vortices. This work highlights the importance of managing transient responses and hysteresis for effective control.

2.3.3. Aeroelastic modeling and characteristics

2.3.3.1. Sweep morphing. Aeroelastic stability is highly sensitive to sweep angle and structural configuration. **Zhang & Zhao (2023)** [147] proposed a time-varying aeroelastic model for rapidly morphing wings, identifying sweep angles as a key factor influencing flutter characteristics. **Wang & Guo (2024)** [132] optimized hinge stiffness for spanwise morphing and sweep angles for sweep morphing, as shown in Fig. 20, increasing critical flutter velocity in high-risk bending angle. **Xie et al. (2024)** [148] further explored supersonic flutter in diamond-back folding wings with ROM, revealing the significant influence of modal shape change on flutter characteristics at a 35° sweep angle and the nonlinear variation trend of local flutter boundary. These studies highlight the interplay between geometric parameters and flutter suppression.

2.3.3.2. Span morphing. Euler-Bernoulli beam theory is frequently adopted for the structural model of span morphing. **Durmuş & Kaya (2021)** [149] modeled a variable-span wing using a coupled bending-torsion Euler-Bernoulli beam and analyzed its free vibration characteristics via the differential transformation method. It is found based on the model that the natural frequencies reduce with span extension.

Various aeroelastic models for span morphing have been established in recent years. **Singha & Murugan (2022)** [150] developed an aeroelastic model based on moving loads of span-morphing wings, modelling

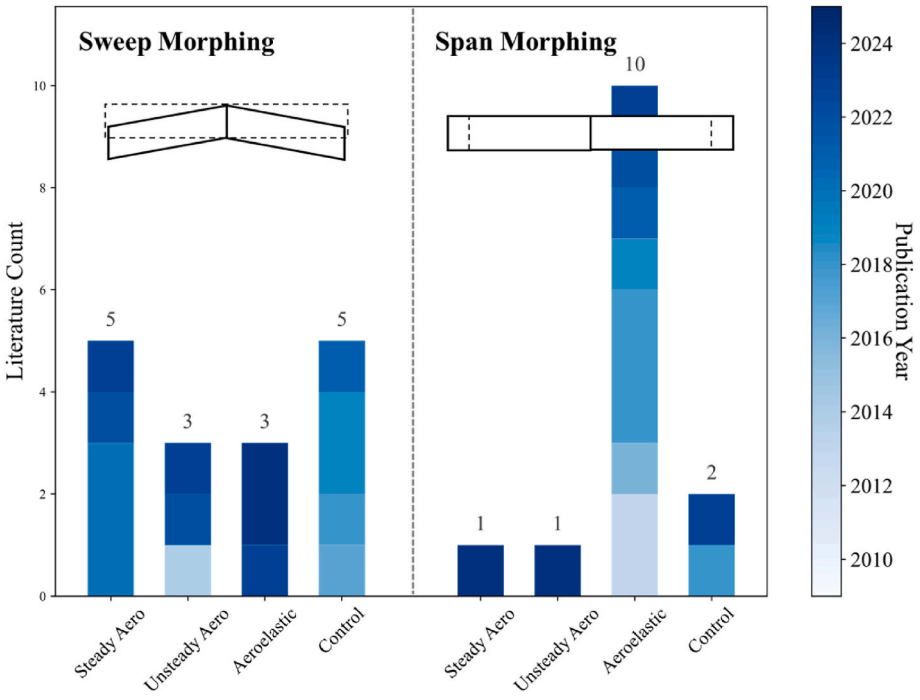

Fig. 17. Literature quantities and publication year at steady, unsteady aerodynamic, aeroelastic, and active control of sweep and span morphing.

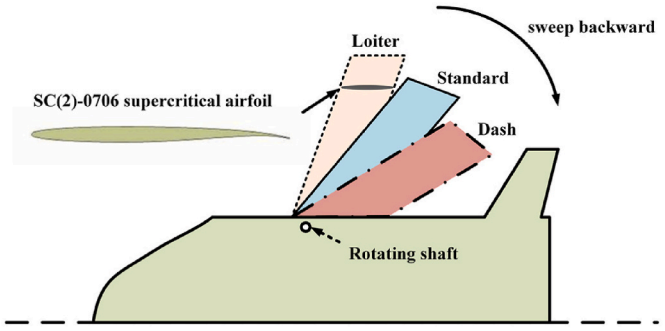

Fig. 18. Sweep morphing strategy [130].

the morphing part as the equivalent moving load acting on the fixed beam. **Huang et al. (2018)** [134] proposed an aeroelastic model incorporating rigid-body motions and flutter analysis. The model is based on unsteady strip aerodynamic theory and Euler-Bernoulli beam theory. **Huang & Qiu (2013)** [135] developed a time-varying state-space model based on Euler-Bernoulli beam theory under time-varying boundary conditions and reduced order unsteady VLM. **Ajaj et al. (2013–2019)** [151–154] proposed a time-domain aeroelastic model based on the Rayleigh-Ritz method and the Theodorsen unsteady aerodynamic theory. For supersonic speed, **Li & Jin (2018)** [155] simplified the variable-span wing as an axial-moving cantilever plate and established a model based on the Kane method and piston theory.

Aeroelastic stability is also a focus point for span morphing, bringing a challenge for its application. Based on the model established, **Huang et al. (2018)** [134] found that span extension shifts flutter mechanisms from bending-torsion coupling to rigid-body modes, reducing flutter velocity by 30%. Moreover, the flutter velocity decreases with span extension. It is also noted by **Huang & Qiu (2013)** [135] that flutter velocity increases with the increase of morphing rate during span extension but decreases during retraction. **Haider et al. (2023)** [136] drew similar conclusions that higher extension rates enhance flutter speeds at specific spans. **Ajaj et al. (2013–2019)** [151–154] investigated the effect of span morphing on flutter suppression. The results demonstrate that flutter suppression can be achieved by span morphing but largely depends on the morphing scheme employed. For supersonic speed, **Li & Jin (2018)** [155] concluded that periodically changing the span length with appropriate amplitude can improve the transient

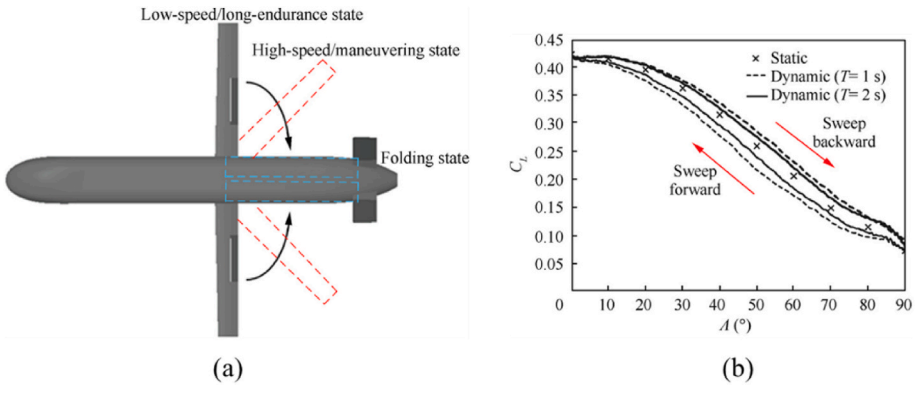

Fig. 19. (a) Wind model [143] (b) numerical results [143].

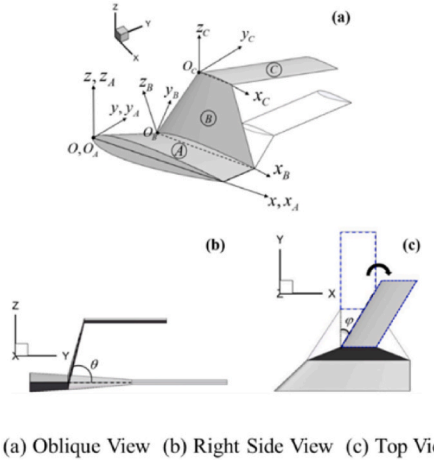

Fig. 20. Spanwise morphing and sweep morphing [132]: (a) oblique, (b) right side, and (c) top view.

stability of the span-morphing aircraft.

Based on the above studies, current research advancements in span morphing demonstrate three aspects:

a) Comprehensive parametric studies have systematically characterized the modal frequency modulation mechanisms inherent to span morphing configurations.
b) Some progress has been made in developing reduced order aeroelastic models for span morphing structures, though existing frameworks predominantly address subsonic flow regimes. Only one study employs the Kane method and piston theory to establish the aeroelastic model of axially morphing cantilever plates for the supersonic condition.
c) Innovative structural architectures for span morphing implementations have been made and undergone aeroelastic stability assessments. However, most studies were either analytical or numerical, and there was a lack of experimental studies. And the nonlinearities with increasing span length have not been considered in current studies.

2.3.4. Active control

2.3.4.1. Sweep morphing. Advanced control strategies are essential to harness the full potential of sweep morphing. Integration of adaptive control frameworks and bio-inspired morphing strategies enhances robustness and simplifies structural complexity. **Yan et al. (2019)** [156] proposed an adaptive super-twisting sliding mode algorithm (ASTA) for trajectory tracking, considering changes of aerodynamic parameters, mass and inertial characteristics during sweep morphing.

Extending this, **Dai et al. (2021)** [157] applied ASTA to a morphing waverider, achieving robust trajectory tracking with significantly lower errors than conventional SMC. **Gao et al. (2018)** [158] achieved pitch and roll control through symmetric and asymmetric sweep morphing in a tandem-wing MAV, validating its control efficacy via a Kane multibody model. **Hui et al. (2019)** [159] mimicked avian wings using bio-inspired discrete sweep morphing, reducing induced drag while improving lateral stability. The UAV achieved an optimal lift-drag ratio and roll control through symmetric and asymmetric wing morphing. **Mallik et al. (2017)** [160] designed a variable-sweep raked wingtip (VGRWT), demonstrating that sweep morphing implements roll control and increases flutter velocity.

2.3.4.2. Span morphing. The symmetric and asymmetric control of span morphing shows great potential in aerodynamic performance optimization and maneuver control. **Ajaj & Jankee (2018)** [131] tested a UAV with symmetric/asymmetric span morphing in wind tunnels, demonstrating that symmetric extensions improve aerodynamic efficiency, while asymmetric morphing generates roll moments with low drag penalties, though slower than conventional ailerons. **Lee et al. (2023)** [161] developed a self-scheduled LPV-based control framework, decoupling symmetric and asymmetric morphing parameters as scheduling parameters and control inputs, respectively.

2.4. Membrane wing

Recent research on membrane wings is primarily driven by the development of MAVs [162], which operate in the low Reynolds number regime (Re = 10^4 to 10^5) like birds and bats. These palm-sized vehicles require high maneuverability and fast adaptation to unsteady flow conditions, which are difficult to achieve with rigid wings due to massive flow separation. While much of the reviewed work focuses on wind-tunnel experiments and high-fidelity simulations to resolve the complex physics of fluid-structure interaction, the goal is to facilitate the design of bio-inspired air vehicles for missions such as sensing and surveillance.

The primary advantage of membrane wings is their ability to passively adapt their camber in response to aerodynamic loads, which leads to significant lift enhancement compared to rigid airfoils [163,164]. At small angles of attack (AoA), the increased camber improves the lift coefficient, while at higher AoAs, the membrane's compliance allows the maximum camber point to shift upwind, effectively delaying stall [165]. Furthermore, self-initiated membrane oscillations in the unsteady regime can excite the shear layer, causing it to roll up into large vortices that further increase mean lift [163].

Modeling membrane-wing aeroelasticity requires coupling structural solvers with fluid dynamics tools. Structurally, researchers use finite difference schemes for simplified 2D or 3D cases or finite element methods (FEM) for complex batten-reinforced or perimeter-reinforced frames [166–168], often employing a corotational framework or p-version Reissner-Mindlin models to account for large displacements and geometric nonlinearities. For the fluid domain, approaches range from robust Reynolds-Averaged Navier-Stokes (RANS) simulations for laminar or steady flows to high-fidelity Large Eddy Simulations (LES/ILES) and Direct Numerical Simulations (DNS), which are essential for capturing the transitional and turbulent scales characteristic of the 10^4-10^5 Reynolds number range [169–172].

The aerodynamic and aeroelastic benefits of membrane wings are shown in Table 5.

3. Analysis frameworks of morphing

In Section 2, a wide variety of morphing technology updates are categorized according to morphing schematics. However, only a limited number of literatures proposed have progressed to the stage of flight validation. As the most rigorous form of verification for morphing technologies, Table 6 summarizes representative morphing aircraft flight tests reported ever since 2010. Among the identified projects, the ACTE program conducted flight tests on a full-scale aircraft platform,

Table 5
Aerodynamic and aeroelastic benefits of membrane wings.

Morphing style	Steady aerodynamics	Unsteady aerodynamics	Aeroelasticity
passive morphing	Lift Enhancement [163,164,173–175] Stall Delay [165,176] Ground Effect Benefits [177,178] Boundary Condition Optimization [179]	Mean Lift Augmentation [163,174] Vortex Control [163,164] Active Actuation Benefits [180,181]	Passive Flow Adaptation [167] Gust Load Alleviation [182,183] Passive Flow Control [184,185]

while the remaining demonstrations were primarily carried out using small UAVs. The limited number of flight demonstrations reflects the technical challenges associated with morphing aircraft, including the power requirements of actuation systems, potential structural weight penalties, limited control authority, and the complexity of integrating morphing mechanisms into reliable flight control architectures.

Camber morphing has achieved the highest level of development and is currently the only configuration demonstrated on a transport-class aircraft [10–13]. In contrast, other morphing concepts remain largely confined to small-scale experimental platforms, which are typically designed to investigate specific performance benefits. Another flight test worth noting is the Lockheed Martin X-56A MUTT program [186] in 2018~2019, which adopts a highly flexible wing with passive deformation. Although not included in Table 6 as morphing aircraft design, the studies on passive deformation of highly flexible wings is fruitful [187–189], which also provide valuable insights for aeroelastic and aeroservoelastic modelling.

Given the limited number of flight demonstrations, most morphing studies remain at the stages of theoretical analysis, numerical simulation, and wind tunnel tests validation. Consequently, accurate and efficient modeling techniques play a critical role in the design and analysis of morphing technologies. This section reviews the principal modeling approaches used in morphing research. The aerodynamic and aeroelastic analysis methods are summarized in Section 3.1 and 3.2. The research on active control, including aeroelastic control, aerodynamic control and maneuver control, is introduced in Section 3.3. The summaries and analyses in this section are based on the work mentioned in Section 2.

3.1. Aerodynamic analysis methods

Aerodynamic modeling often acts as the most computationally demanding component in the analysis and design of morphing aircraft. Compared with conventional aircraft configurations, aerodynamic analysis towards morphing structures introduces additional complexity due to their varying geometries and conjunction with structural modelling. Therefore, aerodynamic analysis for morphing systems involves trade-offs between computational accuracy, numerical cost, and the feasibility of coupling with structural or even control models. The aerodynamic modeling methods used in recent morphing-aircraft studies are summarized in Table 7, which categorizes according to the scope of application and morph schematics. The methods are listed in order of an overall increasing modeling fidelity except for ROM and Other categories.

A notable characteristic of aerodynamic studies in morphing research is the wide spectrum of approaches employed, ranging from low-order potential-flow methods to high-fidelity CFD. In practice, steady aerodynamic analyses are commonly associated with applications such as airfoil optimization, cruise performance evaluation, or conceptual studies of wing-level morphing configurations. In contrast, the use of CFD tends to provide deep insight into the unsteady aerodynamic mechanisms associated with morphing. The distribution of methods across morph schematics also reveals clear tendencies, where lower-fidelity models are predominantly used in wing- or aircraft-level studies, whereas CFD methods are frequently applied to airfoil-level investigations. Among CFD methods, RANS/URANS still dominates the mainstream. This pattern reflects the compromise between accuracy requirements from the unsteady inherence of morphing and the practical complexity of aero-structural coupled modeling.

The group of potential-flow methods frequently used include panel methods, VLM, doublet lattice methods (DLM) and other potential flow-based analytical frameworks. Potential-flow methods are widely adopted in morphing-wing studies due to high computational efficiency and ability to capture the primary aerodynamic characteristics of lifting surfaces. The main assumption is an inviscid and irrotational flow, which allows the velocity field to be expressed as the gradient of a potential function satisfying the Laplace equation:

Table 7
Comparatives of main aerodynamic numerical methods.

Method	Scope of Application	Morph Schematics
VLM/UVLM	Steady [77,79,140,152,153,160], Gust [84,88], Other unsteady [92,105,118,124,135,144]	Twist [77,79,84,118], Span [135,152,153], Sweep [140,144,160], Spanwise [88,105,124], Gull [92,115]
DLM	Steady [123], Flutter [14,109–111,113], Gust [67,89,90], Other unsteady [108,122,132,190,191]	Camber [14,67], Spanwise [89,90,122,123,191], Spanwise [108–111,113,190], Sweep [132]
Panel Method	Steady [6,7,9,10,37–39,50–54,63,65,66,140,153], Gust [125], Flutter [13], Other unsteady [87]	Camber [6,7,9,10,13,37–39,50,53,63,65], Thickness [50–52,54,66], Spanwise [87,125], Sweep [140]
Potential Flow theory[a]	Steady [10,35,86,156], Flutter [43,71], Other unsteady [46,62,117,134,151,154]	Camber [10,35,43,46,62,71,86], Span [134,136,151,154], Sweep [156], Spanwise [86,117]
Euler Equation	Steady [24,64,66], Gust [85]	Camber [24,64,66], Thickness [66], Spanwise [85]
RANS/URANS	Steady [7,17,19,20,23,25,33,39,48–50,53,55,57,64,80,81,83,86,96,97,100,127–129,140,157–159,192], Gust [45,58,68,72–74], Stall [22,26–28,30,34,40,42,44,70], Other unsteady [22,34,36,61,62,94,95,99,101,104,130,133,141,143,145,146]	Camber [7,19,20,22,23,25–28,30,33,34,36,39,40,42,44,45,50,53,57,58,61,62,64,68,70,72–74,86,192], Twist [80,81,83,99,101], Thickness [48–50,55], Spanwise [86,100,104], Dihedral [94–97,127–129], Sweep [130,140,141,143,145,157–159], Span [133,146]
DES/DDES	Stall [34], Other unsteady [34,36,59]	Camber [34,36,59]
DNS	Other unsteady [137–139,142]	Gull [142], Sweep [137–139,142]
Reduced Order Model	Steady [48,55], Stall [44], Gust [84], Other unsteady [148]	Camber [44], Thickness [48,55], Twist [84], Sweep [148], Spanwise [105,106]
Other — Strip theory	Other unsteady [116]	Spanwise [116]
Other — Piston theory	Other unsteady [147,155]	Span [155], Sweep [147]
Other — Laminar NS	Other unsteady [29]	Camber [29]

[a] Here indexes those claimed to model as potential flow but not specified as panel method, VLM or DLM.

Table 6
Morphing techniques into flight tests.

Reference ID	Year	Ground test	Wind tunnel test	Morphing Schematics	Morphing Technique	Speed	Aircraft Weight (kg)
[10,13]	2014, 2015	✓		Camber	Distrubuted compliance	0.3-0.75Ma	16000
[35]	2017		✓	Twist	sliding skin	14-24 m/s	15
[131]	2018		✓	Span	Telescopic Span	15 m/s	15
[16]	2019	✓	✓	Spanwise	Semi Aeroelastic Hinge	25 m/s	19
[119]	2021	✓		Twist, Camber	Sliding skin	Not reported	
[133]	2024	✓		foldable unmanned aerial vehicle	Span-extendable wing	22m/s-29 m/s	10

$$\nabla^2\phi = 0 \tag{1}$$

The aerodynamic solution is typically constructed through the superposition of singularity elements distributed on the lifting surface. Panel methods discretize the body surface with singularity panels and can account for arbitrary three-dimensional geometries, whereas VLM and DLM represent the lifting surface by a lattice of vortices or doublets and are commonly used for steady and unsteady lifting-surface aerodynamics, respectively. The computation of aerodynamic force $\boldsymbol{Q}$ or lift force L through potential flow methods are presented in Table 8. Potential-flow approaches are suitable for attached flows at low to moderate angles of attack, subsonic or weakly compressible flows and moderate morphing amplitudes, where viscous effects and flow separation are negligible. In the context of unsteady aerodynamics, potential-flow methods are used to evaluate aerodynamic load variations under shape deformation, gust response, and flutter. Widely used implementations include XFOIL based on panel method, and ZAERO with DLM for unsteady aeroelastic simulations.

Compared with potential-flow methods, CFD solves the governing equations of viscous compressible flow and performs as a high-fidelity aerodynamic analysis tool. The CFD computation is governed by typical Navier–Stokes (NS) equations[1], and the aerodynamic loads are obtained by integrating the pressure and viscous stresses over surface:

$$\begin{aligned}
&\frac{\partial \rho}{\partial t} + \nabla\cdot(\rho \boldsymbol{u}) = 0 \\
&\frac{\partial (\rho \boldsymbol{u})}{\partial t} + \nabla\cdot(\rho \boldsymbol{u}\boldsymbol{u}) = -\nabla p + \nabla\cdot\boldsymbol{\nu} \\
&\frac{\partial (\rho E)}{\partial t} + \nabla\cdot[(\rho E + p)\boldsymbol{u}] = \nabla\cdot(\boldsymbol{\nu}\cdot\boldsymbol{u}) - \nabla\cdot\boldsymbol{h}
\end{aligned} \tag{2}$$

Within the CFD framework, different turbulence modeling strategies lead to several levels of fidelity and computational cost. Overall, RANS/URANS method is observed to dominate in literature, whereas Euler, DES, and DNS approaches appear only in a small number of studies. RANS/URANS models the average turbulent stresses through turbulence closure models, providing a reasonable balance between accuracy and computational efficiency. In existing studies, RANS/URANS simulations also cover almost all kinds of application scenarios and morphing schematics. In the perspective of morphing schematics, most studies adopting CFD simulation focus on camber deformation, and unsteady simulations appear more frequently than steady analyses.

Higher-fidelity turbulence-resolving approaches have also been explored, but their applications remain limited. DES resolves large-scale turbulent structures while modeling the near-wall turbulence, offering improved accuracy in separated flows but at a significantly higher computational cost. DNS resolves all turbulence scales without modeling assumptions and therefore provides the highest physical fidelity, especially for turbulence modeling, but its computational requirements are still prohibitive for most practical morphing configurations.

For inviscid simulations, the Euler equations are also used in several studies as a simpler CFD-based approach. Euler solvers neglect the viscous term in NS equations and provide moderate computational efficiency. It can capture compressibility effects but cannot accurately predict viscous phenomena involving boundary layers and flow separation. Therefore, it is not as widespread as either RANS/URANS or potential flow-based solvers in the field of morphing aircraft. While CFD methods provide substantially higher accuracy than potential-flow approaches, the computational cost remains a key limitation, particularly when coupled with structural solvers in FSI analyses. In most cases, RANS/URANS-based CFD is generally suggested as the practical level high-fidelity solver currently feasible for most morphing simulations.

A promising approach to alleviating the computational cost in morphing-related FSI simulations and control design is ROM, which aims to construct low-dimensional surrogate models from high-fidelity data. ROM approaches can be broadly classified into physics-based and data-driven categories. Since comprehensive reviews [193–195] of both approaches already exist in the literature, only a brief overview is provided here. Physics-based ROM methods derive reduced models from high-fidelity simulations through modal decomposition and projection techniques, such as proper orthogonal decomposition (POD) and Galerkin projection, which have been widely applied in CFD-based aeroelastic modeling. In contrast, data-driven ROM methods have recently emerged as a rapidly developing research direction, which construct reduced order models directly from simulation or experimental data using system identification or machine-learning techniques, such as dynamic mode decomposition (DMD) and neural networks.

Table 8
Aerodynamic force computation with potential flow-based methods[a].

Scope of application	Aerodynamic equation	Method
Steady	$\boldsymbol{Q} = -\int_S p\boldsymbol{n}dS$	Panel method
	$L = \rho U_\infty \Gamma$	VLM
Unsteady	$\boldsymbol{Q}(t) = \boldsymbol{Q}(\boldsymbol{q}, \dot{\boldsymbol{q}}, t)$	Time-marching potential solvers (Unsteady panel method, UVLM)
	$\boldsymbol{Q}(t) = \int_0^t H(t-\tau)\eta(\tau)d\tau$	Convolution models
	$\boldsymbol{Q}(k) = A(k)\eta(k)$	Frequency domain solvers (DLM)

[a] In Table 8: S – surface area, p – pressure, $\boldsymbol{n}$ – outward unit normal vector, ρ – air density, U_∞ - freestream velocity, Γ – circulation, $\boldsymbol{q}$ – generalized coordinate vector, t – time, $H(t)$ – impulse response function, η – generalized motion variable, τ – time variable, k – reduced frequency, $A(k)$ – influence coefficient matrix.

[1] In Eq., $\boldsymbol{u}$ – velocity vector, E – total energy, $\boldsymbol{\nu}$- viscous stress tensor, $\boldsymbol{h}$ – heat flux.

3.2. Aeroelastic analysis methods

The dynamics of morphing wing aeroelasticity can generally be expressed as the solution of following unified form:

$$\boldsymbol{M}(\boldsymbol{q})\ddot{\boldsymbol{q}} + \boldsymbol{C}(\boldsymbol{q}, \dot{\boldsymbol{q}})\dot{\boldsymbol{q}} + \boldsymbol{K}(\boldsymbol{q}, \dot{\boldsymbol{q}})\boldsymbol{q} + \boldsymbol{N}(\boldsymbol{q}, \dot{\boldsymbol{q}}) = \boldsymbol{Q}[\boldsymbol{q}(\tau), \dot{\boldsymbol{q}}(\tau)]_{\tau\in[0,t]} \tag{3}$$

where each term is defined as follows:

- $\boldsymbol{q}(t)$ denotes the vector of generalized coordinates (modal amplitudes or generalized displacements) obtained through spatial discretization.
- $\boldsymbol{M}(\boldsymbol{q})$ is the generalized inertia operator. In typical applications it reduces to a constant mass matrix, but in more advanced aeroelastic studies it may also incorporate geometric nonlinearities, added-mass contributions, or configuration-dependent coupling with the surrounding fluid. For physically admissible configurations, it remains symmetric and positive definite.
- $\boldsymbol{C}(\boldsymbol{q}, \dot{\boldsymbol{q}})$ represents the structural damping operator. While often modeled as linear viscous damping in simplified aeroelastic analyses, practical studies also account for amplitude- or rate-dependent damping, such as aerodynamic hysteresis, structural friction, or material viscoelasticity. Hence, $\boldsymbol{C}$ can depend on both displacements and velocities.
- $\boldsymbol{K}(\boldsymbol{q}, \dot{\boldsymbol{q}})$ is the structural stiffness operator. In linearized models it is expressed as a constant stiffness matrix $\boldsymbol{K_0}$, whereas in more advanced scenarios it takes a nonlinear form reflecting geometric stiffening, large deflections, or restoring forces from nonlinear mappings.
- $\boldsymbol{N}(\boldsymbol{q}, \dot{\boldsymbol{q}})$ collects additional structural internal nonlinearities not explicitly represented by $\boldsymbol{K}$. This includes mode coupling effects beyond classical stiffness terms, material nonlinearities (e.g.,

plasticity, viscoelasticity), friction and contact effects, or higher-order coupling terms that become significant in large-amplitude aeroelastic responses.

- The right-hand side $\boldsymbol{Q}[\boldsymbol{q}(\tau),\dot{\boldsymbol{q}}(\tau)]_{\tau\in[0,t]}$ indicates the aerodynamic force, mapping the past trajectory up to time t to generalized aerodynamic forces. This is a general representation explicitly admitting causality, hysteresis, irreversible and history-dependent phenomena such as boundary-layer separation, shed wake dynamics, vortex–-structure interaction, and shock motion. The accuracy of this term depends on aerodynamic analysis methods, as introduced in section 3.1.

As discussed in last section, a lot of efforts in current studies have been put into aerodynamic modelling to retain essential fidelity at affordable cost. However, for morphing and highly deformable wings, a substantial portion of the literature focuses on accurately capturing structural nonlinearities and deformation characteristics, which are reflected in the structural operators $\boldsymbol{M}(\boldsymbol{q})$, $\boldsymbol{K}(\boldsymbol{q},\dot{\boldsymbol{q}})$, and the nonlinear term $\boldsymbol{N}(\boldsymbol{q},\dot{\boldsymbol{q}})$ in Eq. (3). In such studies, the aerodynamic model is often simplified using one of the tractable approximations introduced above, allowing the dominant structural effects and their aeroelastic interactions to be more clearly isolated and analyzed. A statistical summary of the structural computation methods employed in existing studies on morphing wings/aircrafts is presented in Table 9.

Structural research on camber morphing is much less extensive than aerodynamic research, and the methods are relatively diverse and dispersed. Different from aerodynamic analysis methods, Table 9 is classified from a complementary workflow of structural physics, spatial discretization, and dynamic solution strategies, which are not mutually exclusive but often used in combination. Among the approaches reported, FEM combined with modal superposition remains the most adopted framework, providing a practical balance between modeling fidelity and computational efficiency for medium-to high-fidelity aeroelastic analysis.

For spanwise and span morphing, the existing literature on aeroelastic analysis demonstrates a pronounced predominance of analytical investigations and numerical methodologies, and there is a lack of experimental studies. The nonlinearity of the structural model is sometimes neglected. The Euler-Bernoulli beam and Rayleigh–Ritz method are applicable to linear models, namely those with small morphing and linear elasticity. However, some studies adopt the CSD methods to consider the structure's nonlinearity. Furthermore, none of the papers in literature has addressed the potential amplification of geometric and aerodynamic nonlinearities with increasing span length, despite their probable significance in span morphing wing configurations.

Table 9
Comparatives of structural numerical methods.

Method		Morph Schematics
Structural physics	Linear elastic beam	Camber [35,46,63,65,71], Spanwise [87, 104,105,107,110,116], Span [134–136, 149,152,154]
Spatial discretization	FEM	Camber [10,13,35,45,46,58,64–67,74], Twist [77,79,118], Spanwise [85, 109–113,115,116,190,191], Thickness [66], Sweep [17,144,147,148,160], Span [136,153]
	FVM	Span [192]
	Rayleigh-Ritz method	Camber [71], Span [151–154]
Dynamic solution	Mode superposition method	Camber [13,14,45,58,67,74], Twist [77, 84], Spanwise [88,106,108,109,117], Span [191]
	Time-domain integration	Camber [44,60,61,70]
	Other CSD	Twist [80–83]

For sweep morphing, structural nonlinearity is taken into consideration in most research. In contrast to aerodynamic modeling, structural nonlinearities do not admit a universal formulation but are instead strongly dependent on the specific configuration, material behavior, and boundary conditions of the structure under study. Typical sources of nonlinearity include large deflections and geometric stiffening effects, material nonlinearities in composites or elastomers, and contact or joint-induced nonlinearities. The use of composite materials further complicates modelling due to their anisotropic stiffness and coupling between bending and torsion. Accurate representation of these effects often requires layered composite modelling or equivalent anisotropic beam formulations. Therefore, structural nonlinear analysis is a problem-dependent modeling process, supported by general numerical frameworks but tailored to the geometry, material, and operational regime of the structure. For example, in a study of a FWT (**Conti et al, 2021**) [191] considering both geometric and hinge-induced nonlinearities, a multi-body formulation is used to describe the system's nonlinear kinematics, and the hinge-induced nonlinearity is described with:

$$\boldsymbol{N}(\boldsymbol{q},\dot{\boldsymbol{q}}) = \boldsymbol{M}(\boldsymbol{q},\dot{\boldsymbol{q}})\ddot{\theta} \tag{4}$$

where $\boldsymbol{M}$ is the coupling mass matrix of hinge, and θ is the hinge rotations.

The final component of aeroelastic modeling concerns the coupling between the aerodynamic and structural analysis subsystems. This coupling determines how the two models exchange information during the simulation, particularly in terms of time advancement and the iteration procedure within each time step. In the computation of aeroelasticity, the FSI frameworks are commonly constructed in loose-coupled or tight-coupled schemes, as shown in Fig. 21. In loose-coupled approaches, the aerodynamic and structural solvers are executed separately, with information exchanged once at discrete time steps. This strategy is widely adopted in practice, especially when strong aerodynamic or structural nonlinearities are involved, such as in simulations involving high-fidelity CFD [45,64]. Tightly coupled frameworks, on the other hand, solve the fluid and structural equations in a more integrated manner, ensuring a higher level of consistency between the two fields at each iteration. However, in many studies adopting this strategy, nonlinear effects are either simplified or neglected to reduce the computational burden. A key challenge of tightly coupled schemes lies in their low computational efficiency, which is often addressed by introducing techniques such as limiting the number of internal iterations, relaxing convergence criteria, or employing adaptive precision control. These measures aim to balance accuracy and stability while keeping the overall cost at an acceptable level. For broader perspectives on fluid–structure interaction and aeroelastic coupling, readers are referred to several classic and comprehensive reviews in the literature [196–199].

3.3. Active control frameworks

Active control via morphing structures enables real-time adaptation to highly dynamic operational environments. The active control via morphing can be divided into aerodynamic control, aeroelastic control and maneuver control, as concluded in Table 10. The active control methods are categorized based on the specific mission objectives into three primary categories: **Aerodynamics**, which mainly focuses on lift-to-drag optimization and stall delay; **Aeroelasticity**, which mainly involves flutter suppression and gust load alleviation and maneuver load alleviation; **Maneuver**, which involves flight mechanics-level transformations for attitude and trajectory tracking.

In the current landscape of morphing aircraft research, camber morph remains the most extensively investigated morphing modality, which is applied across nearly all control objectives. Regarding control law development, open-loop control is adopted at an amount close or marginally surpassing to closed-loop strategies. The adoption of closed-

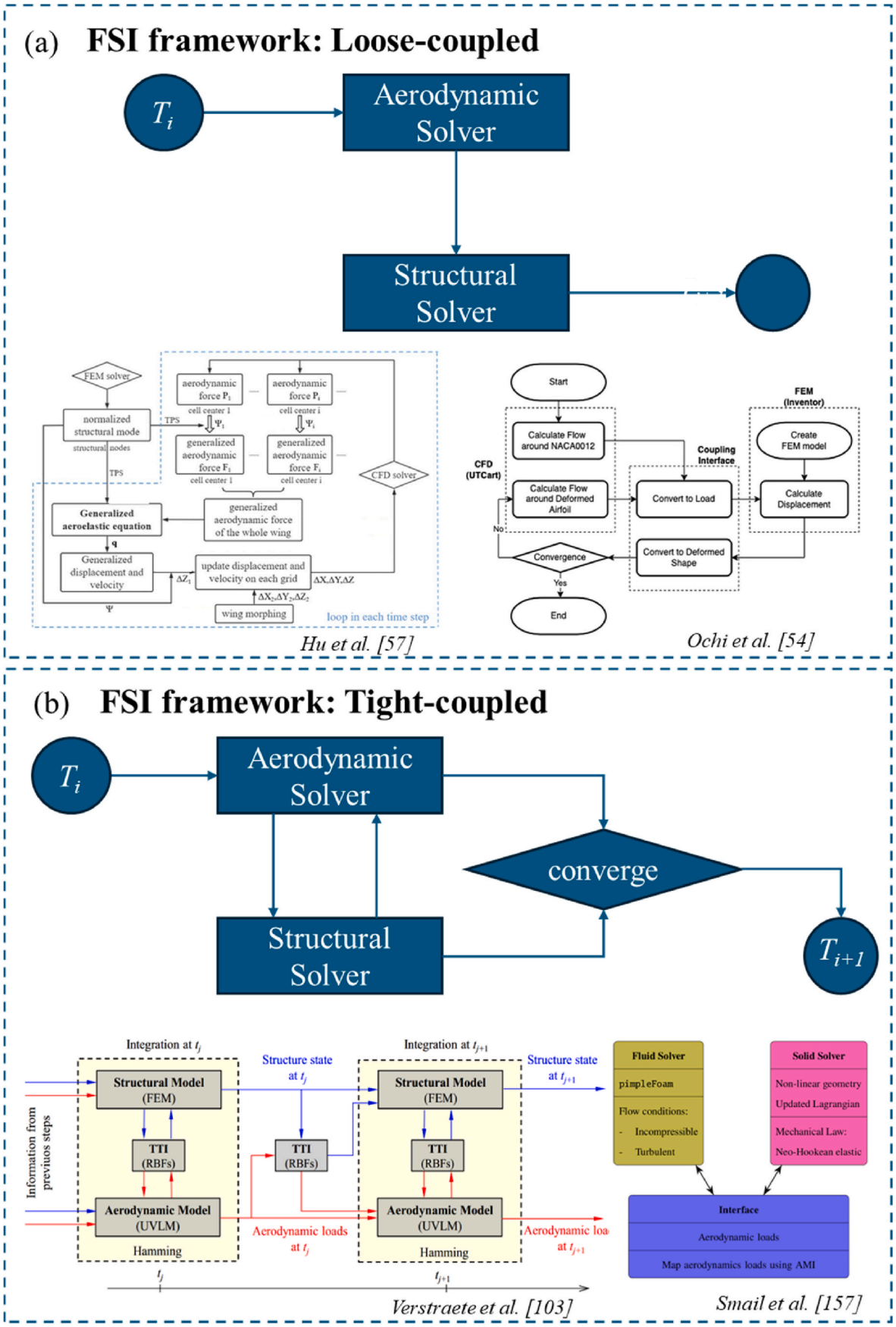

Fig. 21. Typical FSI frameworks: (a) loose-coupled [45,64]; (b) tight-coupled [115,192].

Table 10
Comparatives of Active control methods.

Scope of Application		Morphing schematics	Control law	Validation
Aerodynamics		Camber [26,27,29,30,40–42]	Open-loop [26,27,29,30,40–42]	Simulation [26,27,29,30,40–42], Experiment [41]
Aeroelasticity	Flutter	Camber [44,70,71], Spanwise [125], Span [151–153,155], Sweep [160]	Open-loop [155,160], PID [70], NMI [44], LQR [71]	Model [71], Simulation [44,70,155,160]
	Gust	Camber [45,47,58,67,68,72–74], Spanwise [88–90,114,120,121]	Open-loop [45,58,68,72–74], PID [91], ILAF [67], INDI [47], MDO [74]	Simulation [45,58,68,72–74,88–91], Experiment [47,67,114,121]
	Maneuver load	Camber [46,47], Spanwise [123,124]	Open-loop [46], INDI [46,47]	Model [46], Simulation [123,124], Experiment [47]
Maneuver	Trajectory	Camber [46], Twist [79], Span [161]	Open-loop [46,79], INDI [46], LPV [161]	Model [46,79], Simulation [161]
	Pitch/ Roll/Yaw	Twist [101,118], Sweep [156,158], Gull [93]	Open-loop [93,101], ASTA [156,157], PID [158]	Simulation [101,118,156–158], Experiment [93]

loop methods is currently still hindered by the immense complexity of system design and high cost during computation. For aeroelastic control, a high-fidelity fluid-structure-control interaction (FSCI) framework makes simulation computationally demanding, and sensing requirement in experiment validation is also prohibitive, as shown in Fig. 22.

Currently, most control efficacy validation of current morphing controllers is designed and verified through numerical simulations. A smaller subset of studies employs low-fidelity models for rapid iteration, while a limited number of researchers have achieved physical experimental validation. The validation experiments are confined to ground-based tests or wind tunnel environments. A fully integrated active morphing control system in a flight test environment is not observed. A recent review has provided a comprehensive summary especially concerning morph control, in which various control laws are described in detail [3] (**Parancheerivilakkathil et al, 2024**). Readers may refer to it for further information.

4. Discussion and challenges

An extensive review of aerodynamic and aeroelastic of morphing wing/aircraft in the past decade is presented. To provide a clearer overview of the research landscape, different morphing configurations are further organized in Table 11 according to whether studies on active control, ground experiments, wind tunnel tests, and flight tests have been conducted. The richness of the corresponding literature clearly reflects the maturity and development level of each morphing concept, highlighting the configurations that have progressed from theoretical and numerical investigations toward experimental validation and practical implementation.

The research on camber and spanwise bending morphing is much more comprehensive. Moreover, the investigations on camber morphing focus on steady and unsteady aerodynamic characteristics, while the

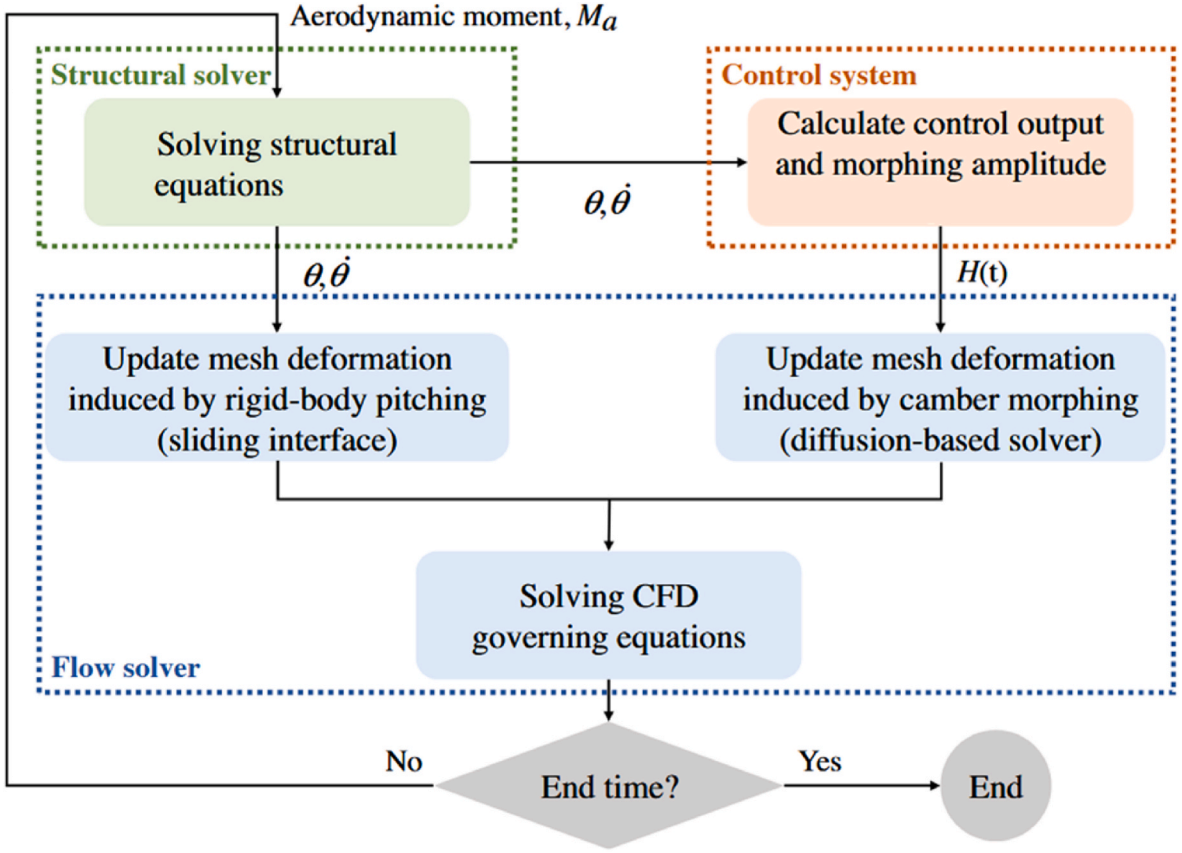

Fig. 22. Control law design framework with loose-coupled FSCI [70].

Table 11
Research updates by morphing schematics.

Morph Schematics	Active Control	Wind Tunnel Test	Ground Test	Flight Test
Camber	[26,30,40–42, 44–47,58,67,68, 70–74]	[8,9,24,31,38, 41,45,47,64, 67]	[10,13,23, 45,56,64, 65]	[10–13, 119]
Thickness		[49,51,54,66]	[66]	
Twist		[35,78,80,82, 99]	[78,119]	[35,119]
Spanwise		[16,91,102, 103,114,121, 126]	[16]	[16]
Gull	[93]	[93]		
Dihedral		[97]		
Sweep	[156–158,160]	[144,146, 159]	[17]	[133, 146]
Span	[155,161]	[131,153]	[153]	[131]

studies on spanwise morphing focus on aeroelastic modelling and characteristics. Because camber morphing directly alters aerodynamic shape, while spanwise morphing significantly affects structural dynamics and stability.

Camber morphing is the most mature and extensively studied morphing configuration, mainly realized through LE and TE deflections that derived from traditional flaps. In the studies of camber morphing, the nonlinearity of structure and aerodynamics have been considered. However, the improvement of substituting traditional flap with camber morphing is seldom clearly discussed. At present, camber morphing is limited to the form of the control surface.

Thickness morphing is currently focused on structural concepts, especially the thermally driven actuation mechanisms based on SMAs. Thickness morphing typically involves deformation in the mid-chord region. While the concept shows potential for intelligent morphing material related applications, its aerodynamic and practical advantages over camber morphing have yet to be fully demonstrated.

Twist and spanwise morphing have progressed to wind tunnel validation in a considerable number of studies. Current research mainly focuses on the nonlinear structural characteristics of these morphing mechanisms, while the investigation of complex aerodynamic mechanisms, such as the coupling between wingtip vortices and wingtip bending, has not been thoroughly investigated. Active control studies in this area are also scarce.

Aircraft-level morphing, including gull, dihedral, sweep and span morphing, is limited due to the low feasibility of the structure. The focus is mainly on steady and quasi-steady studies. Their potential application lies in adjusting the wing configuration in accordance with different working conditions rather than making rapid adjustments. Therefore, there is also little research on strong unsteady aerodynamics computation or tests.

Two structural models are commonly identified in aircraft systems for nonlinear analysis: local and distributed nonlinear structures. The first confines nonlinearity to specific regions, such as joints, enabling linear modeling for the remainder of the system. The second, exemplified by highly flexible wings, involves nonlinearities distributed across most degrees of freedom, necessitating comprehensive geometric or material nonlinear modeling approaches.

The aerodynamic and aeroelastic research methods of morphing include numerical simulation and experimental studies. Except for camber morphing, the numerical simulation mainly adopts low-fidelity numerical models, which ignore the aerodynamic nonlinearity. The experimental studies are mostly conducted through wind tunnel tests, while flight tests are few. Active control via morphing is classified into aerodynamic control, aeroelastic control and maneuver control. The validation approaches for most active control methods are numerical simulations. For morphing strategies that are easy to implement, such as camber morphing and spanwise morphing, the research in the past decade has been more in-depth and has moved closer to application. New works have emerged gradually recently in other morphing schematics. As a promising direction for the future of aircraft, morphing will not be limited to a single type. Currently, research on the integration of multiple morphing strategies is still lacking. There is also a need to further strengthen the research on aeroelastic stability, control effect, reliability, and time-varying aerodynamic performance of a single morphing strategy.

Despite numerous achievements in the analysis of aerodynamic and aeroelastic characteristics of morphing aircraft under various deformation modes, significant challenges persist in addressing the unsteady, nonlinear, fast-response, and high-dimensional modeling arising from continuous morphing. These challenges hinder existing methodologies from comprehensively and effectively dealing with diverse hazardous scenarios and practical requirements in engineering applications.

To be more specific, the main challenges include the following aspects:

(1) *Nonlinearities induced by morphing.* Current research lacks integrated aeroelastic modeling methods capable of simultaneously addressing multiple types of nonlinearities. Most existing studies on the aeroelasticity of morphing wings (particularly focusing on leading and trailing edge morphing) are based on linear assumptions. While a limited number of studies incorporate structural nonlinearities, nonlinear aerodynamic effects are rarely considered. However, in actual flight scenarios, morphing wings simultaneously exhibit various nonlinear factors, including structural nonlinearities, nonlinear aerodynamics, and nonlinearities in the control system, leading to more complex aeroelastic problems. Based on the current state of research, investigations into such issues remain immature and warrant further exploration.

(2) *Effects of actuation system.* Current research primarily focuses on the interaction between structures and aerodynamics, with limited attention given to the influence of actuation systems and deformation rates on the aerodynamic and aeroelastic behavior of morphing wings. With the development of actuator technology, their dynamic characteristics exert increasingly significant effects on the aeroelasticity of flight vehicles. In morphing wing technologies, parameters such as actuation load, rate, and the type of actuation system can substantially impact aeroelastic characteristics. Since aeroelastic behavior is highly dependent on actuator dynamics, actuator nonlinearities may play a critical role in the nonlinear aeroelastic response of the system. However, the sensitivity of the aeroelastic behavior of variable-camber wings to different types of actuation systems has not yet been adequately addressed.

(3) *Time-Varying Aerodynamic Effect.* The morphing process of an aircraft reduces the efficiency of traditional computational methods and introduces nonlinear aerodynamic effects along with local aerodynamic interference issues, so dynamic aerodynamic effect evaluation serves as a key problem of morphing aircraft. During rapid morphing processes, traditional aerodynamic approaches become inadequate for capturing system dynamic behaviors due to the inherent time-varying nature of the system. Therefore, it is necessary to develop time-varying nonlinear aerodynamic models, high-precision real-time rapid evaluation methods, and to develop suitable testing and measurement schemes for morphing aircraft.

(4) *The gap between model and practical application.* The existing research has investigated some aerodynamic and aeroelastic characteristic in simulation modelling, but the actual morphing system has some nonideal factors such as noise and delay, which lead to inaccurate prediction in practical engineering. How to further enhance the model's sophistication and accuracy to meet

the requirements of practical engineering applications remains a challenge.

As conclude, to accelerate the application of possible morphing aircraft, the authors strongly suggest the comprehensively modeling application for design and real fight test of camber morphing aircraft.

CRediT authorship contribution statement

Yuting Dai: Conceptualization, Writing – original draft. **Jinying Li:** Data curation, Investigation. **Yating Hu:** Investigation, Methodology. **Jiaying Zhang:** Writing – review & editing. **Yuming Zhang:** Investigation, Resources. **Ziyan Xi:** Investigation, Writing – review & editing. **Yang Zheng:** Investigation. **Michael I. Friswell:** Supervision, Writing – review & editing.

Declaration of competing interest

The authors declare that they have no known competing financial interests or personal relationships that could have appeared to influence the work reported in this paper.

Acknowledgement

This work was supported by National Natural Science Foundation of China (Grant No. 12472332, and No. U24A2007).

Data availability

No data was used for the research described in the article.

References

[1] Anna-Maria R. McGowan, Dan D. Vicroy, Ronald C. Busan, Andrew S. Hahn, Perspectives on highly adaptive or morphing aircraft. Paper Presented at NATO RTO AVT-168 Symposium, 2009. https://ntrs.nasa.gov/citations/20090017845.
[2] Rafic M. Ajaj, Muhammed S. Parancheerivilakkathil, Mohammadreza Amoozgar, Michael I. Friswell, Wesley J. Cantwell, Recent developments in the aeroelasticity of morphing aircraft, Prog. Aero. Sci. 120 (2021) 100682, https://doi.org/10.1016/j.paerosci.2020.100682.
[3] Muhammed S. Parancheerivilakkathil, et al., A review of control strategies used for morphing aircraft applications, Chin. J. Aeronaut. 37 (4) (2024) 436–463, https://doi.org/10.1016/j.cja.2023.12.035.
[4] Silvestro Barbarino, Onur Bilgen, Rafic M. Ajaj, Michael I. Friswell, Daniel J. Inman, A review of morphing aircraft, J. Intell. Mater. Syst. Struct. 22 (9) (2011) 823–877, https://doi.org/10.1177/1045389X11414084.
[5] Md Najmul Mowla, Davood Asadi, Tahir Durhasan, Javad Rashid Jafari, Mohammadreza Amoozgar, Recent advancements in morphing applications: architecture, artificial intelligence integration, challenges, and future Trends- A comprehensive survey, Aero. Sci. Technol. (2025) 110102, https://doi.org/10.1016/j.ast.2025.110102.
[6] Benjamin King Sutton Woods, Michael I. Friswell, Preliminary investigation of a fishbone active camber concept. Proceedings of the ASME Conference on Smart Materials Adaptive Structures and Intelligent Systems, 2012, pp. 555–563, https://doi.org/10.1115/SMASIS2012-8058.
[7] Benjamin Woods, Aerodynamic modelling of the fish bone active camber morphing concept. The Royal Aeronautical Society Applied Aerodynamics Conference, 2014.
[8] Benjamin Ks Woods, Onur Bilgen, Michael I. Friswell, Wind tunnel testing of the fish bone active camber morphing concept, J. Intell. Mater. Syst. Struct. 25 (7) (2014) 772–785, https://doi.org/10.1177/1045389X14521700.
[9] Andres E. Rivero, Stephane Fournier, Marinos Manolesos, Jonathan E. Cooper, K. S. Woods Benjamin, Experimental aerodynamic comparison of active camber morphing and trailing-edge flaps, AIAA J. 59 (7) (2021) 2627–2640, https://doi.org/10.2514/1.J059606.
[10] Eric J. Miller, William A. Lokos, Josue Cruz, et al., Approach for Structurally Clearing an Adaptive Compliant Trailing Edge Flap for Flight, Society of Flight Test Engineers, 2015. https://ntrs.nasa.gov/citations/20150019388.
[11] S. Kota, R. Osborn, Gregory F. Ervin, Mission adaptive compliant wing – design , fabrication and flight test, RTO Applied Vehicle Technology Panel (AVT) Symposium (2009) 168. https://api.semanticscholar.org/CorpusID:30436033.
[12] Joel Hetrick, et al., Flight testing of mission adaptive compliant wing. 48th AIAA/ASME/ASCE/AHS/ASC Structures, Structural Dynamics, and Materials Conference, 2007, https://doi.org/10.2514/6.2007-1709.
[13] Claudia Y. Herrera, Natalie D. Spivey, Shun-fat Lung, Gregory Ervin, Peter Flick, Aeroelastic Airworthiness Assesment of the Adaptive Compliant Trailing Edge Flaps, Society of Flight Test Engineers, 2015. https://ntrs.nasa.gov/citations/20150020900.
[14] A. Concilio, I. Dimino, R. Pecora, SARISTU: Adaptive Trailing Edge Device (ATED) design process review, Chin. J. Aeronaut. 34 (7) (2021) 187–210, https://doi.org/10.1016/j.cja.2020.08.036.
[15] J.B. Allen, Articulating Winglets, U.S. Patent, 1999 5988563.
[16] Thomas Wilson, James Kirk, John Hobday, Andrea Castrichini, Small Scale flying demonstration of semi aeroelastic hinged wing tips. International Forum on Aeroelasticity and Structural Dynamics, 2019.
[17] Yue Bai, Guang Yang, Hong Xiao, Hongwei Guo, Rongqiang Liu, Bei Liu, An efficient stiffness analysis model based on shear deformation theory for flexible skin shear variable-sweep wing, Chin. J. Aeronaut. 37 (10) (2024) 445–458, https://doi.org/10.1016/j.cja.2024.02.015.
[18] Lingling Chu, Li Qi, Feng Gu, Xintian Du, Yuqing He, Yangchen Deng, Design, modeling, and control of morphing aircraft: a review, Chin. J. Aeronaut. 35 (5) (2022) 220–246, https://doi.org/10.1016/j.cja.2021.09.013.
[19] M. Nemati, A. Jahangirian, Robust aerodynamic morphing shape optimization for high-lift missions, Aero. Sci. Technol. 103 (2020) 105897, https://doi.org/10.1016/j.ast.2020.105897.
[20] Ruochen Wang, Xiaoping Ma, Guoxin Zhang, Ying Pei, Xiangyu Wang, Numerical simulation of continuous morphing wing with leading edge and trailing edge parabolic flaps, J. Aero. Eng. 36 (5) (2023) 04023051, https://doi.org/10.1061/JAEEEZ.ASENG-4622.
[21] Xiaojun Gu, Kaike Yang, Manqiao Wu, Yahui Zhang, Jihong Zhu, Weihong Zhang, Integrated optimization design of smart morphing wing for accurate shape control, Chin. J. Aeronaut. 34 (1) (2021) 135–147, https://doi.org/10.1016/j.cja.2020.08.048.
[22] Zi Kan, Daochun Li, Shen Tong, Jinwu Xiang, Lu Zhang, Aerodynamic characteristics of morphing wing with flexible leading-edge, Chin. J. Aeronaut. 33 (10) (2020) 2610–2619, https://doi.org/10.1016/j.cja.2020.03.012.
[23] Yuzhu Li, Wenjie Ge, Jin Zhou, et al., Design and experiment of concentrated flexibility-based variable camber morphing wing, Chin. J. Aeronaut. 35 (5) (2022) 455–469, https://doi.org/10.1016/j.cja.2021.04.030.
[24] Christopher R. Colletti, Phillip J. Ansell, Airfoil morphed leading-edge design for high-lift applications using genetic algorithm, J. Aircraft 60 (1) (2023) 160–171, https://doi.org/10.2514/1.C036755.
[25] Hector D. Ortiz-Melendez, Ethan Long, Christopher R. Colletti, et al., Design and characterization of high-lift capabilities for slotted, natural-laminar-flow airfoils, J. Aircraft 60 (4) (2023) 1238–1256, https://doi.org/10.2514/1.C037160.
[26] L. Ferrier, M. Vezza, H. Zare-Behtash, Improving the aerodynamic performance of a cycloidal rotor through active compliant morphing, Aeronaut. J. 121 (1241) (2017) 901–915, https://doi.org/10.1017/aer.2017.34.
[27] Chaoyuan Wen, Yuting Dai, Yuntao Xu, Chao Yang, Aerodynamic characteristics of a pitching airfoil with leading-edge morphing, Chin. J. Aeronaut. 37 (7) (2024) 81–92, https://doi.org/10.1016/j.cja.2024.03.036.
[28] M. Bashir, N. Zonzini, S. Longtin Martel, R. Mihaela Botez, A. Ceruti, T. Wong, Numerical investigation of the dynamic stall reduction on the UAS-S45 aerofoil using the optimised aerofoil method, Aeronaut. J. 128 (1321) (2024) 441–468, https://doi.org/10.1017/aer.2023.62.
[29] Wei Kang, Min Xu, Weigang Yao, Jiazhong Zhang, Lock-in mechanism of flow over a low-reynolds-number airfoil with morphing surface, Aero. Sci. Technol. 97 (2020) 105647, https://doi.org/10.1016/j.ast.2019.105647.
[30] Charles M. Hoke, John Young, Joseph C.S. Lai, Enhancing the power-extraction efficiency of a flapping foil by active morphing, AIAA J. 61 (9) (2023) 4056–4069, https://doi.org/10.2514/1.J062291.
[31] Cooper Nelson, Tufan Kumar Guha, Michael Amitay, Control of reverse flow over cantilevered swept blades using passive camber morphing, AIAA J. 62 (4) (2024) 1503–1516, https://doi.org/10.2514/1.J063150.
[32] Rosario Pecora, Morphing wing flaps for large civil aircraft: evolution of a smart technology across the Clean Sky Program, Chin. J. Aeronaut. 34 (7) (2021) 13–28, https://doi.org/10.1016/j.cja.2020.08.004.
[33] Fengqian Hao, Tao Tang, Yuan Gao, Yimeng Li, Shenghui Yi, Jian Lu, Continuous morphing trailing-edge wing concept based on multi-stable nanomaterial, Chin. J. Aeronaut. 34 (7) (2021) 219–231, https://doi.org/10.1016/j.cja.2020.03.041.
[34] Dominic Clements, Kamal Djidjeli, Aerodynamic performance of morphing and periodic trailing-edge morphing airfoils in ground effect, J. Aero. Eng. 36 (3) (2023) 04023012, https://doi.org/10.1061/JAEEEZ.ASENG-4707.
[35] Q. Chanzy, A.J. Keane, Analysis and experimental validation of morphing UAV wings, Aeronaut. J. 122 (1249) (2018) 390–408, https://doi.org/10.1017/aer.2017.130.
[36] W. Zhang, X.T. Nie, X.Y. Gao, W.H. Chen, Conceptual design and Numerical studies of active flow control aerofoil based on shape-memory alloy and macro fibre composites, Aeronaut. J. 125 (1287) (2021) 830–846, https://doi.org/10.1017/aer.2020.135.
[37] J.H.S. Fincham, M.I. Friswell, Aerodynamic optimisation of a camber morphing aerofoil, Aero. Sci. Technol. 43 (2015) 245–255, https://doi.org/10.1016/j.ast.2015.02.023.
[38] R. Wu, C. Soutis, S. Zhong, A. Filippone, A morphing aerofoil with highly controllable aerodynamic performance, Aeronaut. J. 121 (1235) (2017) 54–72, https://doi.org/10.1017/aer.2016.113.
[39] K. Dhileep, D. Kumar, P.N. Gautham Vigneswar, et al., Aerodynamic Study of single corrugated variable-camber morphing aerofoil concept, Aeronaut. J. 126 (1296) (2022) 316–344, https://doi.org/10.1017/aer.2021.71.
[40] Zi Kan, Daochun Li, Jinwu Xiang, Chunxiao Cheng, Delaying stall of morphing wing by periodic trailing-edge deflection, Chin. J. Aeronaut. 33 (2) (2020) 493–500, https://doi.org/10.1016/j.cja.2019.09.028.

[41] Deanna Ko, Tufan Kumar Guha, Michael Amitay, Control of reverse flow over a cantilevered blade using passive camber morphing, AIAA J. 59 (12) (2021) 5310–5331, https://doi.org/10.2514/1.J060229.
[42] You Wu, Yuting Dai, Chao Yang, Yating Hu, Guangjing Huang, Effect of trailing-edge morphing on flow characteristics around a pitching airfoil, AIAA J. 61 (1) (2023) 160–173, https://doi.org/10.2514/1.J061055.
[43] Aqib A. Syed, Mojtaba Moshtaghzadeh, Dewey H. Hodges, Mardanpour Pezhman, Aeroelasticity of flying-wing aircraft subject to morphing: a stability Study, AIAA J. 60 (9) (2022) 5372–5385, https://doi.org/10.2514/1.J061574.
[44] Jinying Li, Yuting Dai, You Wu, Chao Yang, Nonlinear-Model-Inversion control for stall-flutter suppression of an airfoil via camber morphing, AIAA J. 62 (12) (2024) 4665–4681, https://doi.org/10.2514/1.J063907.
[45] Yating Hu, Yuting Dai, You Wu, Chao Yang, Time-Domain feedforward control for gust response alleviation based on seamless morphing wing, AIAA J. 60 (10) (2022) 5707–5722, https://doi.org/10.2514/1.J061763.
[46] Xuerui Wang, Tigran Mkhoyan, Roeland De Breuker, Nonlinear incremental control for flexible aircraft trajectory tracking and load alleviation, J. Guid. Control Dynam. 45 (1) (2022) 39–57, https://doi.org/10.2514/1.G005921.
[47] Xuerui Wang, Tigran Mkhoyan, Iren Mkhoyan, Roeland De Breuker, Seamless active morphing wing simultaneous gust and maneuver load alleviation, J. Guid. Control Dynam. 44 (9) (2021) 1649–1662, https://doi.org/10.2514/1.G005870.
[48] Magalhães Júnior, M. José, Gustavo L.O. Halila, Kyriakos G. Vamvoudakis, Data-Driven controller and multi-gradient search Algorithm for morphing airfoils in high reynolds number flows, Aero. Sci. Technol. 148 (2024) 109106, https://doi.org/10.1016/j.ast.2024.109106.
[49] Martin Robitaille, Mosahebi Ali, Éric Laurendeau, Design of adaptive transonic laminar airfoils using the γ-Re θt transition model, Aero. Sci. Technol. 46 (2015) 60–71, https://doi.org/10.1016/j.ast.2015.06.027.
[50] Chen Liu, Seongkyu Lee, Parametric airfoil design and sensitivity analysis for turbulent boundary-layer trailing-edge noise reduction, AIAA J. 60 (4) (2022) 2324–2341, https://doi.org/10.2514/1.J060096.
[51] Andreea Koreanschi, Oliviu Sugar-Gabor, Mihaela Botez Ruxandra, Numerical and experimental validation of a morphed wing geometry using Price-Païdoussis wind-tunnel testing, Aeronaut. J. 120 (1227) (2016) 757–795, https://doi.org/10.1017/aer.2016.30.
[52] Andreea Koreanschi, Oliviu Sugar-Gabor, Ruxandra Mihaela Botez, Drag optimisation of a wing equipped with a morphing upper surface, Aeronaut. J. 120 (1225) (2016) 473–493, https://doi.org/10.1017/aer.2016.6.
[53] Andrea Magrini, Ernesto Benini, Aerodynamic optimization of a morphing leading edge airfoil with a constant arc length parameterization, J. Aero. Eng. 31 (2) (2018) 04017093, https://doi.org/10.1061/(ASCE)AS.1943-5525.0000812.
[54] Andreea Koreanschi, Oliviu Sugar Gabor, Joran Acotto, et al., Optimization and design of an aircraft's morphing wing-tip demonstrator for drag reduction at low speeds, part II - experimental validation using infra-red transition measurement from wind tunnel tests, Chin. J. Aeronaut. 30 (1) (2017) 164–174, https://doi.org/10.1016/j.cja.2016.12.018.
[55] Magalhães Júnior, M. José, Gustavo L.O. Halila, Yoobin Kim, Thanakorn Khamvilai, Kyriakos G. Vamvoudakis, Intelligent data-driven aerodynamic analysis and optimization of morphing configurations, Aero. Sci. Technol. 121 (2022) 107388, https://doi.org/10.1016/j.ast.2022.107388.
[56] Tianlong Lin, Rosario Pecora, Danilo Ciliberti, Wei Xia, Shuling Hu, Aerodynamic optimization of an adaptive flap for next-generation green aircraft, Chin. J. Aeronaut. 37 (2) (2024) 100–122, https://doi.org/10.1016/j.cja.2023.10.010.
[57] Z.A. Rana, F. Mauret, J.M. Sanchez-Gil, et al., Computational analysis and design of an aerofoil with morphing tail for improved aerodynamic performance in transonic regime, Aeronaut. J. 126 (1301) (2022) 1144–1167, https://doi.org/10.1017/aer.2021.122.
[58] Yuting Dai, Yating Hu, You Wu, Chen Song, Chao Yang, Effect of leading-edge and trailing-edge camber morphing on gust load for an elastic wing, Chin. J. Aeronaut. 38 (4) (2025) 103245, https://doi.org/10.1016/j.cja.2024.09.021.
[59] D. Clements, K. Djidjeli, Periodic morphing of a NACA6409 aerofoil in ground effect, its wake mechanisms and thrust generation, Aeronaut. J. 128 (1330) (2024) 2924–2944, https://doi.org/10.1017/aer.2024.80.
[60] Xiaozhou Fan, Kenneth Breuer, Low-Order modeling of flapping flight with highly articulated, cambered, heavy wings, AIAA J. 60 (2) (2022) 892–901, https://doi.org/10.2514/1.J060661.
[61] Wenzhi Guo, Yongtao Shui, Lu Nie, Gang Chen, Fluid-Structure interaction simulation for multi-body flexible morphing structures, Chin. J. Aeronaut. 37 (2) (2024) 137–147, https://doi.org/10.1016/j.cja.2023.09.009.
[62] Shaobin Li, Zhenxin Tao, Xizhen Song, Unsteady lift model for morphing airfoil based on potential flow theory, Journal of Aerospace Enginerring 31 (2) (2018) 04018006, https://doi.org/10.1061/(ASCE)AS.1943-5525.0000820.
[63] Senthil Murugan, B.K.S. Woods, M.I. Friswell, Hierarchical modeling and optimization of camber morphing airfoil, Aero. Sci. Technol. 42 (2015) 31–38, https://doi.org/10.1016/j.ast.2014.10.019.
[64] Shuji Ochi, Shoko Kai, Kohei Takase, et al., Aeroelastic simulation and experimental validation of a 3D-Printed passive morphing airfoil, AIAA J. 62 (7) (2024) 2538–2547, https://doi.org/10.2514/1.J063000.
[65] Benjamin K.S. Woods, Iman Dayyani, Michael I. Friswell, Fluid/Structure-Interaction analysis of the fish-bone-active-camber morphing concept, J. Aircraft 52 (1) (2015) 307–319, https://doi.org/10.2514/1.C032725.
[66] Cody Wright, Onur Bilgen, Induced-Strain actuators for morphing of multi-element airfoils, J. Aircraft 62 (2) (2025) 409–423, https://doi.org/10.2514/1.C037717.
[67] John Berg, Kuang-Ying Ting, Tyler J. Mundt, Marat Mor, Eli Livne, Kristi A. Morgansen, Exploratory Wind Tunnel Gust Alleviation Tests of a Multiple-Flap Flexible Wing, AIAA Scitech 2020 Forum, 2022, https://doi.org/10.2514/6.2022-2488.
[68] Junaid Ullah, Skander Kamoun Junaid, Jens Müller, Thorsten Lutz, Active Gust Load Alleviation by Means of Steady and Dynamic Trailing and Leading Edge Flap Deflections at Transonic Speeds, AIAA Scitech 2020 Forum, 2022, https://doi.org/10.2514/6.2022-1334.
[69] Jinying Li, Yuting Dai, Yating Hu, Yuming Zhang, Chao Yang, Deep reinforcement learning control for stall flutter via active camber morphing, Phys. Fluids 37 (10) (2025) 105166, https://doi.org/10.1063/5.0295770.
[70] You Wu, Yuting Dai, Chao Yang, Time-Delayed active control of Stall flutter for an airfoil via camber morphing, AIAA J. 60 (10) (2022) 5723–5734, https://doi.org/10.2514/1.J061947.
[71] Jiaying Zhang, Alexander D. Shaw, Chen Wang, et al., Aeroelastic model and analysis of an active camber morphing wing, Aero. Sci. Technol. 111 (2021) 106534, https://doi.org/10.1016/j.ast.2021.106534.
[72] Junaid Ullah, Thorsten Lutz, Lorenz Klug, Rolf Radespiel, Jochen Wild, Ralf Heinrich, Approach for aerodynamic gust load alleviation by means of spanwise-segmented flaps, J. Aircraft 60 (3) (2023) 835–856, https://doi.org/10.2514/1.C037086.
[73] Lorenz Klug, Rolf Radespiel, Junaid Ullah, et al., Actuator Concepts for Active Gust Alleviation on Transport Aircraft at Transonic Speeds, AIAA Scitech 2020 Forum, 2020, https://doi.org/10.2514/6.2020-0271.
[74] Nhan T. Nguyen, Nick B. Cramer, Kelley E. Hashemi, et al., Progress on Gust Load Alleviation Wind Tunnel Experiment and Aeroservoelastic Model Validation for a Flexible Wing with Variable Camber Continuous Trailing Edge Flap System, AIAA Scitech 2020 Forum, 2020, https://doi.org/10.2514/6.2020-0214.
[75] Earl H. Dowell, Donald B. Bliss, Robert L. Clark, Aeroelastic wing with leading- and trailing-edge control surfaces, J. Aircraft 40 (3) (2003) 559–565, https://doi.org/10.2514/2.3130.
[76] P. Zink, Dimitri Mavris, Daniella Raveh, Integrated structural/trim optimization for active aeroelastic wing technology. 8th Symposium on Multidisciplinary Analysis and Optimization, 2000, https://doi.org/10.2514/6.2000-4827.
[77] Erdoğan Kaygan, Ceren Ulusoy, Effectiveness of twist morphing wing on aerodynamic performance and control of an aircraft, Journal of Aviation 2 (2) (2018) 77–86, https://doi.org/10.30518/jav.482507.
[78] Hugo Rodrigue, Seunghyun Cho, Min-Woo Han, Binayak Bhandari, Jae-Eul Shim, Sung-Hoon Ahn, Effect of twist morphing wing segment on aerodynamic performance of UAV, J. Mech. Sci. Technol. 30 (1) (2016) 229–236, https://doi.org/10.1007/s12206-015-1226-3.
[79] John P. Jasa, John T. Hwang, Joaquim R.R. A. Martins, Design and trajectory optimization of a morphing wing aircraft. 2018 AIAA/ASCE/AHS/ASC Structures, Structural Dynamics, and Materials Conference, 2018, https://doi.org/10.2514/6.2018-1382.
[80] N.I. Ismail, A.H. Zulkifli, M.Z. Abdullah, M. Hisyam Basri, Norazharuddin Shah abdullah. "Optimization of Aerodynamic Efficiency for Twist Morphing MAV Wing.", Chin. J. Aeronaut. 27 (3) (2014) 475–487, https://doi.org/10.1016/j.cja.2014.04.017.
[81] N.I. Ismail, A.H. Zulkifli, R.J. Talib, H. Zaini, H. Yusoff, Drag performance of twist morphing MAV wing, MATEC Web of Conferences 82 (2016) 01004, https://doi.org/10.1051/matecconf/20168201004.
[82] N. Ismail, H. Yusoff, Hazim Sharudin, Arif Pahmi, H. Hafi, M.M. Mahadzir, Lift distribution of washout twist morphing MAV wing, Int. J. Eng. Technol. 7 (4) (2018) 89–94, https://doi.org/10.14419/ijet.v7i4.13.21337, 13.
[83] N.I. Ismail, M. Asyraf Tasin, Hazim Sharudin, et al., Computational aerodynamic investigations on wash out twist morphing MAV wings, Evergreen 9 (4) (2022) 1090–1102, https://doi.org/10.5109/6625721.
[84] Majid Ahmadi, Touraj Farsadi, Hamed Haddad Khodaparast, Enhancing gust load alleviation performance in an optimized composite wing using passive wingtip devices: folding and Twist approaches, Aero. Sci. Technol. 147 (2024) 109023, https://doi.org/10.1016/j.ast.2024.109023.
[85] J.E. Cooper, I. Chekkal, R.C.M. Cheung, et al., Design of a morphing wingtip, J. Aircraft 52 (5) (2015) 1394–1403, https://doi.org/10.2514/1.C032861.
[86] João Paulo Eguea, Pedro David Bravo-Mosquera, Fernando Martini Catalano, Camber morphing winglet influence on aircraft drag breakdown and tip vortex structure, Aero. Sci. Technol. 119 (2021) 107148, https://doi.org/10.1016/j.ast.2021.107148.
[87] Pezhman Mardanpour, Dewey H. Hodges, Passive morphing of flying wing aircraft: Z-Shaped configuration, J. Fluid Struct. 44 (2014) 17–30, https://doi.org/10.1016/j.jfluidstructs.2013.09.020.
[88] Andrea Castrichini, et al., Nonlinear folding wing tips for gust loads alleviation, J. Aircraft 53 (5) (2016) 1391–1399, https://doi.org/10.2514/1.C033474.
[89] Andrea Castrichini, et al., Nonlinear negative stiffness wingtip spring device for gust loads alleviation, J. Aircraft 54 (2) (2017) 627–641, https://doi.org/10.2514/1.C033887.
[90] Andrea Castrichini, et al., Preliminary investigation of use of flexible folding wing tips for static and dynamic load alleviation, Aeronaut. J. 121 (1235) (2017) 73–94, https://doi.org/10.1017/aer.2016.108.
[91] Davide Balatti, et al., Active Hinged Wingtip for Gust Load Alleviation and Manoeuvres, AIAA SCITECH, 2023, https://doi.org/10.2514/6.2023-2567, 2023 Forum.
[92] Tianhao Guo, Zhongxi Hou, Zhaowei Liu, Modelling and simulation of flight dynamics for a gull-wing, 2016 IEEE International Conference on Robotics and Biomimetics (ROBIO) (2016) 2181–2186, https://doi.org/10.1109/ROBIO.2016.7866653.
[93] Christina Harvey, Gull wing morphing allows active control of trade-offs in efficiency, maneuverability and stability. Electronic Theses and Dissertations

2008+. T, University of British Columbia, 2018, https://doi.org/10.14288/1.0364534.
[94] Siyuan Chang, Yao Xiao, Guangli Li, Zhongwei Tian, Kai Cui, Numerical Study on hypersonic aerodynamic characteristics of the high-pressure capturing wing configuration with wing dihedral, Aero. Sci. Technol. 143 (2023) 108699, https://doi.org/10.1016/j.ast.2023.108699.
[95] Siyuan Chang, Yao Xiao, Guangli Li, Zhongwei Tian, Kai Cui, Numerical investigation for subsonic performance of the high-pressure capturing wing configuration with wing dihedral, Aero. Sci. Technol. 144 (2024) 108741, https://doi.org/10.1016/j.ast.2023.108741.
[96] Xufei Meng, et al., Low-Speed performance analysis of double swept waverider with wing dihedral, J. Aero. Eng. 38 (2) (2025) 04024124, https://doi.org/10.1061/JAEEEZ.ASENG-5603.
[97] D. Roy, Priyank Kumar, Sudip Das, Effect of anhedral–dihedral angles on 76-40° double-delta wing at low speeds, J. Aero. Eng. 32 (6) (2019) 04019091, https://doi.org/10.1061/(ASCE)AS.1943-5525.0001079.
[98] Hang Zhang, Shenwei Zhang, Tao Xiang, Effects of bio-inspired wing dihedral variations on dynamic soaring performance of unmanned aerial vehicles, Drones 8 (11) (2024) 623, https://doi.org/10.3390/drones8110623.
[99] Kelayeh Karimi, Ruhollah, Mohammad Hassan Djavareshkian, Aerodynamic investigation of twist angle variation based on wing smarting for a flying wing, Chin. J. Aeronaut. 34 (2) (2021) 201–216, https://doi.org/10.1016/j.cja.2020.06.022.
[100] Ali Hussain Kazim, Abdullah Hamid Malik, Hammad Ali, et al., CFD analysis of variable geometric angle winglets, Aircraft Eng. Aero. Technol. 94 (2) (2022) 289–301, https://doi.org/10.1108/AEAT-10-2020-0241.
[101] Kelayeh Karimi, Ruhollah, Mohammad Hasan Djavareshkian, Aerodynamic assessment of a control strategy based on twist morphing wing in a flying wing aircraft, J. Aero. Eng. 37 (1) (2024) 04023087, https://doi.org/10.1061/JAEEEZ.ASENG-5073.
[102] Kamlesh Joshi, Bhattacharya Samik, The unsteady force response of an accelerating flat plate with controlled spanwise bending, J. Fluid Mech. 933 (2022) A56, https://doi.org/10.1017/jfm.2021.1110.
[103] Kun Jia, Scofield Tyler, Wei Mingjun, Samik Bhattacharya, Vorticity transfer in a leading-edge vortex due to controlled spanwise bending, Phys. Rev. Fluids 6 (2) (2021) 024703, https://doi.org/10.1103/PhysRevFluids.6.024703.
[104] Yuting Dai, Yingjie Xia, Guangjing Huang, Chao Yang, Yongchang Li, Performance improvement of a wing with a controlled spanwise bending wingtip, Ocean. Eng. 287 (2023) 115795, https://doi.org/10.1016/j.oceaneng.2023.115795.
[105] R. De Breuker, M. Abdalla, Z. Gürdal, Design of morphing winglets with the inclusion of nonlinear aeroelastic effects, Aeronaut. J. 115 (1174) (2011) 713–728, https://doi.org/10.1017/S0001924000006461.
[106] Wei Hu, Zhichun Yang, Yingsong Gu, Aeroelastic Study for folding wing during the morphing process, J. Sound Vib. 365 (2016) 216–229, https://doi.org/10.1016/j.jsv.2015.11.043.
[107] T. Wilson, A. Azabal, A. Castrichini, J. Cooper, R. Ajaj, M. Herring, Aeroelastic behaviour of hinged wing tips. 5th Aircraft Structural Design Conference, Royal Aeronautical Society, 2016, 2016, http://eprints.soton.ac.uk/id/eprint/400895.
[108] Yingge Ni, Chi Hou, Xiaopeng Wan, Meiying Zhao, Transient aeroelastic responses of folding wing in morphing motion. International Conference on Advances in Mechanical Engineering and Industrial Informatics, 2015, https://doi.org/10.2991/ameii-15.2015.253.
[109] Wei Zhang, Shengli Lv, Yingge Ni, Parametric aeroelastic modeling based on component modal synthesis and stability analysis for horizontally folding wing with Hinge joints, Nonlinear Dyn. 92 (2) (2018) 169–179, https://doi.org/10.1007/s11071-017-3956-5.
[110] Matthew P. Snyder, Brian Sanders, Franklin E. Eastep, Geoffrey J. Frank, Vibration and flutter characteristics of a folding wing, J. Aircraft 46 (3) (2009) 791–799, https://doi.org/10.2514/1.34685.
[111] Yonghui Zhao, Haiyan Hu, Parameterized aeroelastic modeling and flutter analysis for a folding wing, J. Sound Vib. 331 (2) (2012) 308–324, https://doi.org/10.1016/j.jsv.2011.08.028.
[112] Yonghui Zhao, Haiyan Hu, Prediction of transient responses of a folding wing during the morphing process, Aero. Sci. Technol. 24 (1) (2013) 89–94, https://doi.org/10.1016/j.ast.2011.09.001.
[113] Yoo Yeon Jung, Ji Hwan Kim, Aeroelastic behavior of morphing wing in flutter regions, Appl. Mech. Mater. 284 (2013) 442–445. https://doi.org/10.4028/www.scientific.net/AMM.284-287.442.
[114] Ronald CM. Cheung, et al., Testing of a hinged wingtip device for gust loads alleviation, J. Aircraft 55 (5) (2018) 2050–2067, https://doi.org/10.2514/1.C034811.
[115] Marcos L. Verstraete, Bruno A. Roccia, Dean T. Mook, Preidikman Sergio, A Co-Simulation methodology to simulate the nonlinear aeroelastic behavior of a folding-wing concept in different flight configurations, Nonlinear Dyn. 98 (2) (2019) 907–927, https://doi.org/10.1007/s11071-019-05234-9.
[116] Sebastian Liska, Earl H. Dowell, Continuum aeroelastic model for a folding-wing configuration, AIAA J. 47 (10) (2009) 2350–2358, https://doi.org/10.2514/1.40475.
[117] Ivan Wang, S. Chad Gibbs, Earl H. Dowell, Aeroelastic model of multisegmented folding wings: theory and experiment, J. Aircraft 49 (3) (2012) 911–921, https://doi.org/10.2514/1.C031589.
[118] R. Pecora, F. Amoroso, L. Lecce, Effectiveness of wing twist morphing in roll control, J. Aircraft 49 (6) (2012) 1666–1674, https://doi.org/10.2514/1.C000328.
[119] Vale Lobo do, José, John Raffaelli, Afzal Suleman, Experimental validation and evaluation of a coupled twist-camber morphing wing concept, Appl. Sci. 11 (22) (2021) 10631, https://doi.org/10.3390/app112210631.
[120] Thomas Wilson, et al., Aircraft wing with a moveable wing tip device for load alleviation, U.S. Patent (2021) 11203410.
[121] Ronald C. Cheung, Djamel Rezgui, Jonathan E. Cooper, Thomas Wilson, Testing of folding wing-tip for gust load alleviation in high aspect ratio wing, AIAA Scitech 2019 Forum (2019), https://doi.org/10.2514/6.2019-1863.
[122] Andrea Castrichini, et al., Aeroelastics flight dynamics coupling effects of the semi-aeroelastic Hinge device, J. Aircraft 57 (2) (2020) 333–341, https://doi.org/10.2514/1.C035602.
[123] Federico Fonte, et al., Active load control of a regional aircraft wing equipped with morphing winglets. Smart Materials, Adaptive Structures and Intelligent Systems 51944, 2018, https://doi.org/10.1115/SMASIS2018-8167.
[124] Rafic M. Ajaj, Flight dynamics of transport aircraft equipped with flared-hinge folding wingtips, J. Aircraft 58 (1) (2021) 98–110, https://doi.org/10.2514/1.C035940.
[125] Davide Balatti, et al., The effect of folding wingtips on the worst-case gust loads of a simplified aircraft model, Proc. Inst. Mech. Eng. G J. Aerosp. Eng. 236 (2) (2022) 219–237, https://doi.org/10.1177/09544100211010915.
[126] Zhuoer Yao, Zi Kan, Daochun Li, Gust response of spanwise morphing wing by simulation and wind tunnel testing, Aerospace 10 (4) (2023) 328, https://doi.org/10.3390/aerospace10040328.
[127] Liu Chuanzhen, Meng Xufei, Bai Peng, Design and analysis of double-swept waverider with wing dihedral, AIAA J. 60 (4) (2022) 2075–2084, https://doi.org/10.2514/1.J060706.
[128] Siyuan Chang, Yao Xiao, Guangli Li, Zhongwei Tian, Kai Cui, Numerical Study on hypersonic aerodynamic characteristics of the high-pressure capturing wing configuration with wing dihedral, Aero. Sci. Technol. 143 (2023) 108699, https://doi.org/10.1016/j.ast.2023.108699.
[129] Siyuan Chang, Yao Xiao, Guangli Li, Zhongwei Tian, Kai Cui, Numerical investigation for subsonic performance of the high-pressure capturing wing configuration with wing dihedral, Aero. Sci. Technol. 144 (2024) 108741, https://doi.org/10.1016/j.ast.2023.108741.
[130] Pei Dai, et al., Design and aerodynamic performance analysis of a variable-sweep-wing morphing waverider, Aero. Sci. Technol. 98 (2020) 105703, https://doi.org/10.1016/j.ast.2020.105703.
[131] Rafic M. Ajaj, K. Jankee Girish, The Transformer aircraft: a multimission unmanned aerial vehicle capable of symmetric and asymmetric span morphing, Aero. Sci. Technol. 76 (2018) 512–522, https://doi.org/10.1016/j.ast.2018.02.022.
[132] Jin-Gang Wang, Xiang-Ying Guo, Research on the flutter characteristics of folding wings with variable swept angles of the outer wing, Aero. Sci. Technol. 155 (2024) 109685, https://doi.org/10.1016/j.ast.2024.109685.
[133] Peng Si, Mingjian Wu, Yongqing Huo, Zhilin Wu, Investigation on improving aerodynamics and flight performance for an unmanned aircraft with a span-extendable wing, Aero. Sci. Technol. 145 (2024) 108905, https://doi.org/10.1016/j.ast.2024.108905.
[134] Chao Huang, et al., Variations of flutter mechanism of a span-morphing wing involving rigid-body motions, Chin. J. Aeronaut. 31 (3) (2018) 490–497, https://doi.org/10.1016/j.cja.2017.12.014.
[135] Ren Huang, Zhiping Qiu, Transient aeroelastic responses and flutter analysis of a variable-span wing during the morphing process, Chin. J. Aeronaut. 26 (6) (2013) 1430–1438, https://doi.org/10.1016/j.cja.2013.07.047.
[136] Z. Haider, R.M. Ajaj, L. Seneviratne, On the effect of morphing rate on aeroelastic dynamic stability of a polymorphing wing, Aerospace 10 (1) (2023) 57, https://doi.org/10.3390/aerospace10010057.
[137] Kai Zhang, et al., Laminar separated flows over finite-aspect-ratio swept wings, J. Fluid Mech. 905 (2020) R1, https://doi.org/10.1017/jfm.2020.778.
[138] Jean Hélder Marques Ribeiro, et al., Wing sweep effects on laminar separated flows, J. Fluid Mech. 950 (2022) A23, https://doi.org/10.1017/jfm.2022.612.
[139] JH Marques Ribeiro, Chi-An Yeh, Kunihiko Taira, Triglobal resolvent analysis of swept-wing wakes, J. Fluid Mech. 954 (2023) A42, https://doi.org/10.1017/jfm.2022.1033.
[140] M. Elelwi, et al., Comparison and analyses of a variable span-morphing of the tapered wing with a varying sweep angle, Aeronaut. J. 124 (1278) (2020) 1146–1169, https://doi.org/10.1017/aer.2020.19.
[141] Han Han, Jun Hu, Yong Yu, Investigation of the unsteady aerodynamic characteristics of an unmanned aerial vehicle with variable-sweep morphing. 32nd AIAA Applied Aerodynamics Conference, 2014, https://doi.org/10.2514/6.2014-3130.
[142] Chunyu Wang, et al., Aerodynamic performance of a bio-inspired flapping wing with local sweep morphing, Phys. Fluids 34 (5) (2022), https://doi.org/10.1063/5.0090718.
[143] Lifang Zeng, et al., Mechanism analysis of hysteretic aerodynamic characteristics on variable-sweep wings, Chin. J. Aeronaut. 36 (5) (2023) 212–222, https://doi.org/10.1016/j.cja.2023.01.002.
[144] Yue Bai, et al., An unsteady aerodynamic force calculation method for shear variable-sweep wing considering sweep angle and airfoil changes, Aero. Sci. Technol. 157 (2025) 109771, https://doi.org/10.1016/j.ast.2024.109771.
[145] Ziyan Xi, et al., Aerodynamic investigation and modeling of dynamic variable sweep wing at low Reynolds number, Phys. Fluids 37 (3) (2025), https://doi.org/10.1063/5.0255492.
[146] Peng Si, Mingjian Wu, Yongqing Huo, Zhilin Wu, Investigation on the transient aerodynamics of a tube-launched unmanned aerial vehicle with a span-extended

wing, J. Phys. Conf. 2820 (1) (2024) 012074, https://doi.org/10.1088/1742-6596/2820/1/012074.
[147] Liqi Zhang, Yonghui Zhao, Time-Varying aeroelastic modeling and analysis of a rapidly morphing wing, Aerospace 10 (2) (2023) 197, https://doi.org/10.3390/aerospace10020197.
[148] Pengze Xie, et al., Supersonic flutter mechanism of "diamond-back" folding wings, Aero. Sci. Technol. 153 (2024) 109396, https://doi.org/10.1016/j.ast.2024.109396.
[149] Damla Durmuş, Metin O. Kaya, Free vibration characteristics of a variable-span morphing wing. International Symposium on Sustainable Aviation, Springer International Publishing, Cham, 2021, https://doi.org/10.1007/978-3-031-37943-7_3.
[150] Debashis Singha, Senthil Murugan, Aeroelastic Analysis of a Span Morphing Wing with Moving Loads, AIAA Scitech, 2022, https://doi.org/10.2514/6.2022-1124. Forum. 2022.
[151] Rafic M. Ajaj, Michael I. Friswell, Aeroelasticity of compliant span morphing wings, Smart Mater. Struct. 27 (10) (2018) 105052, https://doi.org/10.1088/1361-665X/aad219.
[152] R.M. Ajaj, E.I. Saavedra Flores, M.I. Friswell, et al., The Zigzag wingbox for a span morphing wing, Aero. Sci. Technol. 28 (1) (2013) 364–375, https://doi.org/10.1016/j.ast.2012.12.002.
[153] R.M. Ajaj, M.I. Friswell, M. Bourchak, W. Harasani, Span morphing using the GNATSpar wing, Aero. Sci. Technol. 53 (2016) 38–46, https://doi.org/10.1016/j.ast.2016.03.009.
[154] Rafic M. Ajaj, et al., Flutter of telescopic span morphing wings, Int. J. Struct. Stabil. Dynam. 19 (6) (2019) 1950061, https://doi.org/10.1142/S0219455419500615.
[155] Wencheng Li, Dongping Jin, Flutter suppression and stability analysis for a variable-span wing via morphing technology, J. Sound Vib. 412 (2018) 410–423, https://doi.org/10.1016/j.jsv.2017.10.009.
[156] Binbin Yan, et al., Adaptive super-twisting sliding mode control of variable sweep morphing aircraft, Aero. Sci. Technol. 92 (2019) 198–210, https://doi.org/10.1016/j.ast.2019.05.063.
[157] Pei Dai, et al., Longitudinal tracking control for a morphing waverider using adaptive super twisting control, IEEE Access 9 (2021) 59692–59702, https://doi.org/10.1109/ACCESS.2021.3073401.
[158] Liang Gao, Hongzhe Jin, Jie Zhao, Hegao Cai, Yanhe Zhu, Flight dynamics modeling and control of a novel catapult launched Tandem-Wing Micro Aerial Vehicle with variable sweep, IEEE Access 6 (2018) 42294–42308, https://doi.org/10.1109/ACCESS.2018.2858293.
[159] Zhe Hui, Yang Zhang, Gang Chen, Aerodynamic performance investigation on a morphing unmanned aerial vehicle with bio-inspired discrete wing structures, Aero. Sci. Technol. 95 (2019) 105419, https://doi.org/10.1016/j.ast.2019.105419.
[160] Wrik Mallik, Rakesh K. Kapania, Joseph A. Schetz, Aeroelastic applications of a variable-geometry raked wingtip, J. Aircraft 54 (1) (2017) 62–74, https://doi.org/10.2514/1.C033805.
[161] Jihoon Lee, et al., Self-Scheduled LPV control of asymmetric variable-span morphing UAV, Sensors 23 (6) (2023) 3075, https://doi.org/10.3390/s23063075.
[162] Sonya Tiomkin, Daniella E. Raveh, A review of membrane-wing aeroelasticity, Prog. Aero. Sci. 126 (2021) 100738, https://doi.org/10.1016/j.paerosci.2021.100738.
[163] Raymond E. Gordnier, High fidelity computational simulation of a membrane wing airfoil, J. Fluid Struct. 25 (5) (2009) 897–917, https://doi.org/10.1016/j.jfluidstructs.2009.03.004.
[164] Pinunta Rojratsirikul, Zhijin Wang, Ismet Gursul, Unsteady fluid–structure interactions of membrane airfoils at low Reynolds numbers, Exp. Fluid 46 (5) (2009) 859–872, https://doi.org/10.1007/s00348-009-0623-8.
[165] Masato Okamoto, Kunio Yasuda, Akira Azuma, Aerodynamic characteristics of the wings and body of a dragonfly, J. Exp. Biol. 199 (2) (1996) 281–294, https://doi.org/10.1242/jeb.199.2.281.
[166] Sonia Serrano-Galiano, Neil D. Sandham, Richard D. Sandberg, Fluid–structure coupling mechanism and its aerodynamic effect on membrane aerofoils, J. Fluid Mech. 848 (2018) 1127–1156, https://doi.org/10.1017/jfm.2018.398.
[167] S. Tiomkin, D.E. Raveh, On membrane-wing stability in laminar flow, J. Fluid Struct. 91 (2019) 102694, https://doi.org/10.1016/j.jfluidstructs.2019.102694.
[168] Bret Stanford, et al., Fixed membrane wings for micro air vehicles: experimental characterization, numerical modeling, and tailoring, Prog. Aero. Sci. 44 (4) (2008) 258–294, https://doi.org/10.1016/j.paerosci.2008.03.001.
[169] Heng Xiao, Cinnella Paola, Quantification of model uncertainty in RANS simulations: a review, Prog. Aero. Sci. 108 (2019) 1–31, https://doi.org/10.1016/j.paerosci.2018.10.001.
[170] Philippe R. Spalart, Detached-eddy simulation, Annu. Rev. Fluid Mech. 41 (1) (2009) 181–202, https://doi.org/10.1146/annurev.fluid.010908.165130.
[171] Miguel Visbal, P. Morgan, D. Rizzetta, An implicit LES approach based on high-order compact differencing and filtering schemes. 16th AIAA Computational Fluid Dynamics Conference, 2003, https://doi.org/10.2514/6.2003-4098.
[172] Bret Stanford, et al., Static aeroelastic model validation of membrane micro air vehicle wings, AIAA J. 45 (12) (2007) 2828–2837, https://doi.org/10.2514/1.30003.
[173] Sonya Tiomkin, Daniella Raveh, Rimon Arieli, Parametric study of a two-dimensional membrane wing in viscous laminar flow. 29th AIAA Applied Aerodynamics Conference, 2011, https://doi.org/10.2514/6.2011-3023.
[174] Arnold Song, et al., Aeromechanics of membrane wings with implications for animal flight, AIAA J. 46 (8) (2008) 2096–2106, https://doi.org/10.2514/1.36694.
[175] Pinunta Rojratsirikul, Zhijin Wang, Ismet Gursul, Effect of pre-strain and excess length on unsteady fluid–structure interactions of membrane airfoils, J. Fluid Struct. 26 (3) (2010) 359–376, https://doi.org/10.1016/j.jfluidstructs.2010.01.005.
[176] Jack N. Nielsen, Theory of flexible aerodynamic surfaces, 435-442, https://doi.org/10.1115/1.3636575, 1963.
[177] Robert Bleischwitz, Roeland De Kat, Bharathram Ganapathisubramani, Aeromechanics of membrane and rigid wings in and out of ground-effect at moderate Reynolds numbers, J. Fluid Struct. 62 (2016) 318–331, https://doi.org/10.1016/j.jfluidstructs.2016.02.005.
[178] Robert Bleischwitz, Roeland De Kat, Bharathram Ganapathisubramani, On the fluid-structure interaction of flexible membrane wings for MAVs in and out of ground-effect, J. Fluid Struct. 70 (2017) 214–234, https://doi.org/10.1016/j.jfluidstructs.2016.12.001.
[179] Robert Bleischwitz, Roeland de Kat, Bharathram Ganapathisubramani, Aspect-ratio effects on aeromechanics of membrane wings at moderate Reynolds numbers, AIAA J. 53 (3) (2015) 780–788, https://doi.org/10.2514/1.J053522.
[180] Michael R. Hays, et al., Aerodynamic control of micro air vehicle wings using electroactive membranes, J. Intell. Mater. Syst. Struct. 24 (7) (2013) 862–878, https://doi.org/10.1177/1045389X12470303.
[181] Oscar M. Curet, et al., Aerodynamic characterization of a wing membrane with variable compliance, AIAA J. 52 (8) (2014) 1749–1756, https://doi.org/10.2514/1.J052688.
[182] Wei Shyy, et al., Computational aerodynamics of low Reynolds number plunging, pitching and flexible wings for MAV applications, Acta Mech. Sin. 24 (4) (2008) 351–373, https://doi.org/10.1007/s10409-008-0164-z.
[183] Raymond E. Gordnier, J. Attar Peter, Impact of flexibility on the aerodynamics of an aspect ratio two membrane wing, J. Fluid Struct. 45 (2014) 138–152, https://doi.org/10.1016/j.jfluidstructs.2013.10.004.
[184] Yongsheng Lian, et al., Membrane wing aerodynamics for micro air vehicles, Prog. Aero. Sci. 39 (6-7) (2003) 425–465, https://doi.org/10.1016/S0376-0421(03)00076-9.
[185] Yongsheng Lian, Wei Shyy, Laminar-turbulent transition of a low Reynolds number rigid or flexible airfoil, AIAA J. 45 (7) (2007) 1501–1513, https://doi.org/10.2514/1.25812.
[186] Jacob Schaefer, Peter Suh, Matt Boucher, Jeff Ouellette, Alex Chin, Chris Miller, Jared Grauer, Greg Reich, Robert Mitchell, Pete Flick, Flying beyond flutter with the X-56A aircraft, NASA Report (2023) 20220012337. https://ntrs.nasa.gov/citations/20220012337.
[187] Or Avin, Daniella E. Raveh, Ariel Drachinsky, Yaron Ben-Shmuel, Moshe Tur, Experimental aeroelastic benchmark of a very flexible wing, AIAA J. 60 (3) (2022) 1745–1768, https://doi.org/10.2514/1.J060621.
[188] Cristina Riso, Carlos E.S. Cesnik, Impact of low-order modeling on aeroelastic predictions for very flexible wings, J. Aircraft 60 (3) (2023) 662–687, https://doi.org/10.2514/1.C036869.
[189] André F.P. Ribeiro, Damiano Casalino, Carlos Ferreira, Free wake Panel method simulations of a highly flexible wing in flutter and gusts, J. Fluid Struct. 121 (2023) 103955, https://doi.org/10.1016/j.jfluidstructs.2023.103955.
[190] Peicheng Li, Yingge Ni, Chi Hou, Xiaopeng Wan, Meiying Zhao, Nonlinear aeroelastic modeling of a folding wing structure, J. Phys. Conf. 1215 (1) (2019) 012009, https://doi.org/10.1088/1742-6596/1215/1/012009.
[191] Claudio Conti, et al., Quasi-Steady aeroelastic analysis of the semi-aeroelastic Hinge including geometric nonlinearities, J. Aircraft 58 (5) (2021) 1168–1178, https://doi.org/10.2514/1.C036115.
[192] Smail Boughou, et al., Investigation on aeroelasticity of morphing wing through dynamic response and virtual structural damping, Phys. Fluids 36 (9) (2024) 091902, https://doi.org/10.1063/5.0223164.
[193] Mehdi Ghoreyshi, Adam Jirasek, Russell M. Cummings, Reduced order unsteady aerodynamic modeling for stability and control analysis using computational fluid dynamics, Prog. Aero. Sci. 71 (2014) 167–217, https://doi.org/10.1016/j.paerosci.2014.09.001.
[194] Jiaqing Kou, Weiwei Zhang, Data-driven modeling for unsteady aerodynamics and aeroelasticity, Prog. Aero. Sci. 125 (2021) 100725, https://doi.org/10.1016/j.paerosci.2021.100725.
[195] Steven L. Brunton, J. Nathan Kutz, Data-Driven Science and Engineering: Machine Learning, Dynamical Systems, and Control, second ed., Cambridge University Press, Cambridge, 2022 https://doi.org/10.1017/9781009089517.
[196] Earl H. Dowell, Kenneth C. Hall, Modeling of fluid-structure interaction, Annu. Rev. Fluid Mech. 33 (1) (2001) 445–490, https://doi.org/10.1146/annurev.fluid.33.1.445.
[197] Ramji Kamakoti, Wei Shyy, Fluid–structure interaction for aeroelastic applications, Prog. Aero. Sci. 40 (8) (2004) 535–558, https://doi.org/10.1016/j.paerosci.2005.01.001.
[198] Tayfun E. Tezduyar, Sathe Sunil, Modelling of fluid–structure interactions with the space–time finite elements: solution techniques, Int. J. Numer. Methods Fluid. 54 (6) (2007) 855–900, https://doi.org/10.1002/fld.1430, 8.
[199] Gene Hou, Jin Wang, Anita Layton, Numerical methods for fluid-structure interaction—a review, Commun. Comput. Phys. 12 (2) (2012) 337–377, https://doi.org/10.4208/cicp.291210.290411s.